

CYCLIC PERFORMANCE AND STRENGTHENING OF BUILT-UP BATTENED
COLUMNS

ABDUL WAHEED

A thesis submitted in fulfilment of the
requirements for the award of the degree of
Doctor of Philosophy

School of Civil Engineering
Faculty of Engineering
Universiti Teknologi Malaysia

AUGUST 2022

DEDICATION

I would like to dedicate this thesis to my beloved parents for their endless support and encouragement.

ACKNOWLEDGEMENT

In the name of Allah, the most beneficent and the most merciful In preparing this thesis, I was in contact with many people, researchers, and academicians. They have contributed towards my understanding and thoughts. In particular, I wish to express my sincere appreciation to my main thesis supervisor, Associate Professor Dr. Mohammadreza Vafaei, for encouragement, guidance, critics and friendship. I am also very thankful to my co-supervisor Associate Professor Dr. Sophia C. Alih for her guidance, advices and motivation. Without their continued support and interest, this thesis would not have been the same as presented here. I have learned from them not only how to perform and interpret experiments but also how to think and move the project forward. My sincere appreciation also extends to all my colleagues and others who have provided assistance at various occasions. Their views and tips are useful indeed. Unfortunately, it is not possible to list all of them in this limited space. Finally, yet importantly, I would like to express utmost appreciation to my lovely and kind parents and wife for their love, support and encouragements throughout my life.

ABSTRACT

Built-up battened columns have been widely used in steel structures mainly because of providing a higher moment of inertia than solid sections with a similar weight. Despite wide application in steel constructions, the seismic design of these columns has not been well addressed in the literature, and seismic design codes do not provide a specific seismic design guideline for them. On the other hand, past earthquakes have shown that built-up battened columns have been vulnerable against seismic actions mainly because of the plastic deformation in battens, fracture of battens, global buckling of columns, local buckling of web and flanges, and formation of plastic hinges at their bottom panel. Therefore, their seismic behaviour should be investigated, and an efficient strengthening method should be proposed. In this study, experimental works and numerical simulations were conducted to investigate the governing failure modes of built-up batten columns. Besides, the effect of batten's thickness, battens spacing, chord distance and axial load on the ultimate load, ductility ratio, stiffness degradation rate and energy dissipation capacity of built-up battened columns were investigated through quasi-static cyclic loading. This study also proposed a strengthening method through the filling of chords with grout and wrapping it with carbon fibre reinforced polymer (CFRP). Experimental works included four unstrengthen and four strengthened columns with different battens spacing and chord distances. Besides, 210 built-up battened columns with different batten thicknesses, battens spacing, chord distances, axial forces, number of CFRPs layers and number of strengthened panels were simulated in ABAQUS software and subjected to cyclic loading. The obtained results indicated that the bulging of chord webs together with the local buckling of chord flanges were the main reason for the failure of columns. Moreover, built-up columns did not reach their plastic moment capacity because of local buckling in flanges. Furthermore, the columns with 62 mm batten spacing showed a 30% larger ultimate load than that of the column with 550 mm batten spacing. The results also indicated that the columns with 62 mm batten spacing reached 95.91% of their theoretical bending capacity. It was shown that design codes' requirements for batten spacing was not conservative and did not result in an identical safety margin for the bending moment capacity of built-up columns. An increase in the chord distance from 50 mm to 150 mm enhanced the lateral strength of the column by 35%. On the other hand, an increase in the axial force from $0.1F_y$ to $0.4F_y$ decreased the lateral strength and ultimate displacement by 24% and 36%, respectively. The displacement ductility ratios of the unstrengthen built-up battened columns were less than two even when subjected to an axial compression ratio smaller than 0.2. The results indicated that CFRP application delays/shifts the local buckling of flanges and bulging of the web to the upper un-retrofitted panels; however, an increase in the number of CFRPs layers did not show any pronounced effect. The retrofitting of columns resulted in a significant increase in the lateral strength and corresponding displacement by 32.15% and 39.34%, respectively, as compared to the un-retrofitted columns. The energy dissipation capacity of retrofitted columns was 66.39% higher than that of the un-retrofitted columns. The retrofitted columns lost 27%, while the un-retrofitted columns lost 52% of their initial lateral stiffness at a drift ratio of 5.0%. In addition, the retrofitted columns were also able to reach their plastic moment capacity and had a displacement ductility ratio larger than two. The outcome of this study helps practice engineers to understand the seismic behavior of built-up battened columns better and provides an efficient retrofitting method for these columns.

ABSTRAK

Tiang bertetulang terbina telah digunakan secara meluas dalam struktur keluli terutamanya kerana ia memberikan momen inersia yang lebih tinggi berbanding seksyen pejal dengan berat yang sama. Walaupun aplikasinya meluas dalam pembinaan keluli, reka bentuk seismik untuk tiang ini tidak dihurai dengan mendalam dalam literatur, dan kod reka bentuk seismik tidak menyediakan garis panduan reka bentuk seismik khusus untuknya. Sebaliknya, gempa bumi yang lalu telah menunjukkan bahawa tiang bertetulang terbina adalah berisiko terhadap beban seismik terutamanya disebabkan oleh ubah bentuk plastik dalam tetulang, keretakan tetulang, lengkokan global tiang, lengkokan tempatan pada web dan bebibir, dan pembentukan plastik engsel pada panel bawahnya. Oleh itu, tingkah laku seismik mereka harus disiasat, dan kaedah pengukuhan yang cekap harus dicadangkan. Dalam kajian ini, kerja eksperimen dan simulasi berangka telah dijalankan untuk menyiasat mod kegagalan yang mengawal tiang bertetulang terbina. Selain itu, kesan ketebalan tetulang, jarak tetulang, jarak kord dan beban paksi ke atas beban muktamad, nisbah kemuluran, kadar degradasi kekakuan dan kapasiti pelepasan tenaga tiang bertetulang terbina telah disiasat melalui pemuatan kitaran separa statik. Kajian ini juga mencadangkan kaedah pengukuhan melalui pengisian grout di dalam kord dan pembalut polimer bertetulang gentian karbon (CFRP) pada kord tiang bertetulang terbina. Kerja-kerja eksperimen termasuk empat tiang yang tidak dikukuhkan dan empat tiang yang diperkukuh dengan jarak tetulang dan jarak kord yang berbeza. Selain itu, 210 tiang bertetulang terbina dengan ketebalan tetulang yang berbeza, jarak tetulang, jarak kord, daya paksi, bilangan lapisan CFRP dan bilangan panel yang diperkukuh telah disimulasikan dalam perisian ABAQUS dan tertakluk kepada beban kitaran. Keputusan yang diperolehi menunjukkan bahawa pembonjolan jaringan kord bersama-sama lekuk tempatan bebibir kord adalah sebab utama kegagalan tiang. Selain itu, tiang bertetulang terbina tidak mencapai kapasiti momen plastiknya kerana lengkokan tempatan dalam bebibir. Tambahan pula, tiang dengan jarak tetulang 62 mm menunjukkan beban muktamad 30% lebih besar daripada tiang dengan jarak tetulang 550 mm. Keputusan juga menunjukkan bahawa tiang dengan jarak tetulang 62 mm mencapai 95.91% daripada kapasiti lenturan teorinya. Ia ditunjukkan bahawa keperluan kod reka bentuk untuk jarak tetulang yang tidak konservatif dan tidak menghasilkan margin keselamatan yang sama untuk kapasiti momen lentur tiang bertetulang terbina. Peningkatan jarak kord daripada 50 mm kepada 150 mm meningkatkan kekuatan sisi lajur sebanyak 35%. Sebaliknya, peningkatan daya paksi daripada $0.1F_y$ kepada $0.4F_y$ mengurangkan kekuatan sisi dan anjakan muktamad masing-masing sebanyak 24% dan 36%. Nisbah kemuluran anjakan bagi tiang bertetulang terbina yang tidak teguh adalah kurang daripada dua walaupun tertakluk kepada nisbah mampatan paksi yang lebih kecil daripada 0.2. Keputusan menunjukkan bahawa aplikasi CFRP melambatkan/mengalihkan lekuk tempatan bebibir dan membonjolkan jaringan ke panel atas yang tidak diubahsuai; walau bagaimanapun, peningkatan dalam bilangan lapisan CFRP tidak menunjukkan sebarang kesan yang ketara. Pengubahsuaian tiang menghasilkan peningkatan yang ketara dalam kekuatan sisi dan anjakan yang sepadan masing-masing sebanyak 32.15% dan 39.34%, berbanding tiang yang tidak diubahsuai. Kapasiti pelepasan tenaga tiang yang diubahsuai adalah 66.39% lebih tinggi daripada tiang yang tidak diubahsuai. Tiang yang diubahsuai kehilangan 27%, manakala tiang yang tidak diubahsuai semula kehilangan 52% daripada kekakuan sisinya pada nisbah hanyutan 5.0%. Di samping itu, tiang yang diubahsuai juga dapat mencapai kapasiti momen plastiknya dan memberikan nisbah kemuluran anjakan lebih daripada dua. Hasil kajian ini membantu jurutera latihan untuk memahami tingkah laku seismik tiang berbatang terbina dengan lebih baik dan menyediakan kaedah pengubahsuaian yang cekap untuk tiang ini.

TABLE OF CONTENTS

	TITLE	PAGE
	DECLARATION	iii
	DEDICATION	iv
	ACKNOWLEDGEMENT	v
	ABSTRACT	vi
	ABSTRAK	vii
	TABLE OF CONTENTS	viii
	LIST OF TABLES	xiv
	LIST OF FIGURES	xv
	LIST OF ABBREVIATIONS	xxv
	LIST OF SYMBOLS	xxvi
	LIST OF APPENDICES	xxviii
CHAPTER 1	INTRODUCTION	1
1.1	Problem Statement	7
1.2	Research Objectives	9
1.3	Scope of the study	10
1.4	Significance of the study	10
1.5	Layout of Thesis	11
CHAPTER 2	LITERATURE REVIEW	15
2.1	Introduction	15
2.2	Built-up Columns	16
2.3	Ductility and Energy Dissipation	19
2.4	Previous Research Studies on Built-up Columns	21
2.4.1	Shear Effect and Slenderness Ratio	21
2.4.2	Compound Buckling and Initial Imperfections	23
2.4.3	Effect of Sectional Slenderness	25
2.5	Performance of Built-up Columns	28

2.5.1	Axial Performance	28
2.5.2	Cyclic Performance of Built-Up Columns	32
2.5.2.1	Battened Columns	32
2.5.2.2	Laced Columns	37
2.6	Design Approached in various codes	38
2.7	Composite Constructions	43
2.7.1	Static Behaviour of Composite Columns	46
2.7.2	Cyclic Performance of composite columns	49
2.7.3	Design Guidelines for Composite Construction	52
2.8	Retrofitting of Structural systems using FRPs	53
2.8.1	Traditional retrofitting techniques	53
2.8.2	Retrofitting of structures by FRPs	54
2.8.3	Types and Methods of FRPs Installation	54
2.8.4	Behaviour of Retrofitted Sections	57
2.8.4.1	Axial Response	57
2.8.4.2	Flexural Response	66
2.8.4.3	Impact Response	77
2.9	Summary	79
CHAPTER 3	METHODOLOGY OF EXPERIMENTAL WORK	85
3.1	Introduction	85
3.2	Experimental work	85
3.2.1	Determination of size and number of test specimens	86
3.2.2	Fabrication of test specimen	91
3.2.3	Preparation and filing of SkiaGrout-215	93
3.2.4	Installation of CFRP	95
3.2.5	Test set up and loading of test specimens	97
3.2.6	Material test	101
3.2.6.1	Tensile strength test of steel	101
3.2.6.2	Compressive strength test of SikaGrout-215	104

	3.2.6.3	Modulus of Elasticity (E) and Poisson ratio (ν)	105
	3.2.6.4	Technical characteristics of (CFRP) and epoxy resin	106
3.3		Summary	107
CHAPTER 4		EXPERIMENTAL TEST RESULTS	109
4.1		Introduction	109
4.2		Results of experimental tests	109
	4.2.1	Un-retrofitted built-up battened columns	109
	4.2.1.1	Test Observations and Failure Modes	111
	4.2.1.2	Hysteretic response	117
	4.2.1.3	Backbone curve	119
	4.2.1.4	Stiffness Degradation	123
	4.2.1.5	Energy Dissipation	125
	4.2.1.6	Strain measurements	127
	4.2.1.7	Summary of experimental results obtained for the un-retrofitted columns	129
	4.2.2	Retrofitted built-up battened columns	130
	4.2.2.1	Test Observations and Failure Modes	130
	4.2.2.2	Hysteretic response	140
	4.2.2.3	Backbone curve	143
	4.2.2.4	Stiffness degradation	145
	4.2.2.5	Energy dissipation	148
	4.2.2.6	Strain measurement	149
	4.2.2.7	Summary of experimental results obtained for the retrofitted columns	152
4.3		Comparison between results of retrofitted and un-retrofitted columns	153
	4.3.1	Failure Modes	153
	4.3.2	Backbone curve	157
	4.3.3	Ultimate strength	159

4.3.4	Stiffness degradation	159
4.3.5	Energy dissipation	162
4.3.6	Strain measurement	163
4.4	Summary	166
CHAPTER 5	NUMERICAL STUDIES	169
5.1	Introduction	169
5.2	Finite element simulation	169
5.2.1	Parts creation	171
5.2.2	Determination of Material properties	171
5.2.3	Parts Assembling	173
5.2.4	Interaction and boundary conditions	174
5.2.5	Finite Element Type and Meshing	175
5.2.5.1	Mesh size sensitivity	177
5.2.6	Analysis Steps and Load application	178
5.2.6.1	Modelling of Initial Global and local geometric imperfections	178
5.3	Validation of the finite element model	179
5.4	Parametric study of un-retrofitted specimens	182
5.4.1	Failure modes of simulated columns	184
5.4.1.1	Stress distribution	189
5.4.2	Effect of batten thickness on the cyclic response of the column	192
5.4.2.1	Hysteresis loops and backbone curves	192
5.4.3	Effect of batten spacing on the cyclic response of columns	194
5.4.3.1	Hysteresis loops and backbone curves	194
5.4.3.2	Ultimate loads	200
5.4.3.3	Displacement ductility ratios	203
5.4.3.4	Energy dissipation	205
5.4.3.5	Stiffness degradation	209

5.4.4	Effect of chord distance on the cyclic response of the columns	211
5.4.4.1	Hysteresis loops and backbone curves	211
5.4.4.2	Ultimate loads and ultimate displacement	213
5.4.4.3	Displacement ductility ratios	214
5.4.4.4	Energy dissipation	215
5.4.4.5	Stiffness degradation	218
5.4.5	Effect of axial force on the cyclic response of column	219
5.4.5.1	Hysteresis loops and backbone curves	219
5.4.5.2	Ultimate loads and ultimate displacements	223
5.4.5.3	Displacement ductility ratio	224
5.4.5.4	Energy dissipation	226
5.4.5.5	Stiffness degradation	229
5.4.6	Summary of the numerical results obtained for the un-retrofitted columns	231
5.5	Parametric study of retrofitted columns	233
5.5.1	Effect of CFRP retrofitting on the cyclic response of columns	233
5.5.1.1	Validation of finite element model	233
5.5.1.2	Failure modes of retrofitted columns	235
5.5.1.3	Hysteresis loops and backbone curves	240
5.5.1.4	Ultimate loads and ultimate displacements	246
5.5.1.5	Displacement ductility ratio	252
5.5.1.6	Energy dissipation	254
5.5.1.7	Stiffness degradation	260
5.5.2	Summary of the numerical results obtained for the retrofitted columns	265

CHAPTER 6	CONCLUSIONS AND RECOMMENDATIONS	269
6.1	Conclusions	269
6.1.1	First objective - Governing failure modes	269
6.1.2	Second objective	270
6.1.3	Third objective - Effect of axial force	271
6.1.4	Fourth objective - Cyclic performance of retrofitted columns	271
6.2	Contribution to the body of knowledge	272
6.3	Recommendation for future works	273
REFERENCES		275
APPENDICES		293
LIST OF PUBLICATIONS		325

LIST OF TABLES

TABLE NO.	TITLE	PAGE
Table 2.1	Limiting width to thickness ratios (14)(52)	26
Table 2.2	Summary of the past research of built-up columns	81
Table 3.1	Details of tested samples	89
Table 3.2	Mechanical properties of test specimens	91
Table 3.3	Dimension of tensile test coupons	102
Table 3.4	Measured material properties obtained from tensile coupon test	104
Table 3.5	Determination of modulus elasticity and poison ratio	106
Table 3.6	Technical propertied of the employed CFRP and epoxy resin	106
Table 4.1	Structural characteristics of the tested samples	122
Table 4.2	Structural characteristics of the retrofitted tested samples	145
Table 5.1	Parameters used in the finite element model of the column	172
Table 5.2	Results of sensitivity analysis conducted on the mesh size of battens and chords	177
Table 5.3	Details of specimens for the numerical simulation of the second objective	183
Table 5.4	Details of specimens with constant battens thickness for the numerical simulation of the third objective	183
Table 5.5	Details of specimens for the numerical simulation of the fourth objective	183
Table 5.6	Stress in flanges at the onset of local buckling	203
Table 5.7	Bending moment capacities of retrofitted columns	249

LIST OF FIGURES

FIGURE NO.	TITLE	PAGE
Figure 1.1	Column failure modes	4
Figure 1.2	Types of built-up (a) battened columns (b) laced columns	6
Figure 1.3	Types of built-up sections (a) channels face-to-face (b) channels back-to-back (c) I-sections (d) angle section (continue)	7
Figure 1.4	Failure modes of built-up battened columns (11)	8
Figure 1.5	Research methodology flow chart	13
Figure 2.1	Overview of the literature review	16
Figure 2.2	Built-up columns (a) Battened column (b) Laced column	18
Figure 2.3	Different types of Ductility (32)	20
Figure 2.4	Failure modes (a) local flexural buckling (b) flexural torsional (54)(55)(56)	27
Figure 2.5	Configuration of built-up battened columns (a) fasteners pattern (b) type of batten plates (79)	31
Figure 2.6	Failure modes of specimen (a) conventional spacing of battens (b) reduced spacing of battens at end panel (c) boxing at end panel (8)(9)	33
Figure 2.7	Failure location of (a) DCFF sections (b) DCBB sections (c) DI sections (10)	35
Figure 2.8	Modes of failure (a) B35-E12-P1 (b) B35-E12-P3 (c) B35-E8-P1 (d) B25-E12-P1 (81)	36
Figure 2.9	Buckling of flanges and web (a) chord distance 8 cm (b) chord distance 12 cm (83)	37
Figure 2.10	Composite columns: (a) Encasement of structural steel in concrete, (b) Steel tube filled by concrete and reinforcement bar, (c) Steel tube filled by concrete (CFT), (d) Structural steel shape fully encased in CFT and (e) Structural steel shape partially encased in reinforced concrete	44
Figure 2.11	Schematic failure modes of hollow steel tube, concrete and concrete-filled steel tube (91)	45

Figure 2.12	Deformation at the impact location (a) hollow section (b) concrete filled section (103)	47
Figure 2.13	Behaviour of CFT columns (a) compressive strength (b) axial shortening (91)	48
Figure 2.14	Failure modes of (a) Inward and outward buckling of hollow square section (b) Outward buckling of square sections (c) Inward buckling of inner circular section (19)	50
Figure 2.15	Restraining mechanism of concrete and cyclic loading (20)	51
Figure 2.16	External wrapping of CFRP	56
Figure 2.17	Strengthened specimen configuration (117)	59
Figure 2.18	Strengthening of sections through mortar FRP fabrics (118)	59
Figure 2.19	Modes of buckling of bare and strengthened sections (138)	61
Figure 2.20	Failure modes of specimen (a) unconfined (b) fully confined (c) partially confined (139)	62
Figure 2.21	Wrapping of CFRP layers (141)	63
Figure 2.22	Failure modes of tested samples (a) outward buckling (b) tearing of steel tube (c) local buckling of rectangular section (d) local buckling of square section (e) fracture of CFRP rectangular section (f) fracture of CFRP square section (141)	65
Figure 2.23	Strengthened section (a) schematic diagram (b) test specimen (142)	66
Figure 2.24	Effectiveness of CFRP in controlling local buckling and torsional buckling (a) un-strengthened (b) only flanges strengthened (c) global buckling of un-strengthened (d) specimen with strengthened web and flanges (21)(22)	67
Figure 2.25	Researched specimen (a) Uni and Bi directional skin CFRP wrap, (b) Uni directional closed CFRP wrap, (c) Bi directional closed CFRP wrap(120)(121)(122)	69
Figure 2.26	Failure of specimens (a) without CFRP (b) with surface CFRP (c) with infill material and surface CFRP (120)(121)(122)	70
Figure 2.27	Different failure modes of CFRP (a) delamination (b) rupture (c) wrinkles in CFRP (119)	71
Figure 2.28	Tested samples: (a) control sample; (b) retrofitted with 1.5-mm-thick channel; (c) retrofitted with 2.5-mm-thick channel; and (d) details of welding (143)	72

Figure 2.29	Schematic view of FRPs strengthened CHS (23)	73
Figure 2.30	Tested samples (a) before testing (b) after testing (23)	73
Figure 2.31	Failure modes of bare and retrofitted samples (123)	74
Figure 2.32	Failure modes of (a) bare section (b) strengthened section (124)	75
Figure 2.33	Bare (BF) and strengthened steel frames (SF) for testing (149)	76
Figure 2.34	Failure modes of (a) unconfined columns (b) confined columns (150)	77
Figure 2.35	Failure modes (a) control (b) 2 sides CFRP (c) 4 sides CFRP (152)	78
Figure 2.36	Failure modes of tested bare and strengthened circular hollow sections (CHS) (153)	79
Figure 3.1	Flow chart of the methodology for experimental work	86
Figure 3.2	Behaviour of column with subjected to lateral loading	88
Figure 3.3	Schematic view of test sample. (a) Battens spacing 550 mm (b) Battens spacing 225 mm	89
Figure 3.4	Fabricated specimens in workshop	92
Figure 3.5	Painting of test specimens	92
Figure 3.6	Specimens with (a) two strain gauge (b) four strain gauge	93
Figure 3.7	Test specimens of Group-II (a) grouting (b) surface of hardened grout	94
Figure 3.8	Installation of CFRP sheet (a) epoxy resin (b) specimen wrapped with CFRP	97
Figure 3.9	Schematic diagram of overall experimental setup	99
Figure 3.10	Test setup	100
Figure 3.11	Employed loading protocol (156)	100
Figure 3.12	Data recording and loading setup	101
Figure 3.13	Tensile test specimen	102
Figure 3.14	Tensile testing of coupons	103
Figure 3.15	Tested samples from (a) channels section (b) batten plates	103
Figure 3.16	Tested sika grout cubes	104

Figure 3.17	Modulus of elasticity test (a) sample inside machine (b) samples after test	105
Figure 4.1	Flow chart of experimental results	110
Figure 4.2	Failure modes of specimen U-D50-S225	113
Figure 4.3	Failure modes of specimen U-D100-S225	114
Figure 4.4	Observed damages to specimen U-D50-S500	115
Figure 4.5	Observed damages to the specimen U-D100-S550	116
Figure 4.6	Hysteresis loops of specimens (a) U-D50-S225 (b) U-D50-S550 (c) U-D100-S225 (d) U-D100-S550	119
Figure 4.7	Backbone curves of specimens (a) U-D50-S225 (b) U-D50-S550 (c) U-D100-S225 (d) U-D100-S550	121
Figure 4.8	Bilinear representation of the backbone curve	122
Figure 4.9	Comparison among the stiffness degradation of specimens (a) U-D50-S225 (b) U-D50-S550 (c) U-D100-S225 (d) U-D100-S550	124
Figure 4.10	Energy dissipation ability of specimens (a) U-D50-S225 (b) U-D50-S550 (c) U-D100-S225 (d) U-D100-S550	126
Figure 4.11	Measured web strains (a) Push direction (b) Pull direction	128
Figure 4.12	Measured strains of specimen U-D100-S225 (a) Strain ratio (web/flange) (b) strain in flanges	129
Figure 4.13	Observed damage to R-D50-S225 (a) no visible damage (b) no visible damage (c) no visible damage (d) initiation of outward bulging (e) outward bulging (f) outward bulging (g) left chord bulging (h) right chord bulging	133
Figure 4.14	Observed damage to R-D100-S225 (a) no visible damage (b) no visible damage (c) no visible damage (d) initiation of outward bulging (e) stress concentration (f) outward bulging (g) left chord bulging (h) right chord bulging (continue)	135
Figure 4.15	Observed damage to R-D50-S550	138
Figure 4.16	Observed damage to R-D100-S550	140
Figure 4.17	Hysteresis loops of retrofitted specimens (a) R-D50-S225 (b) R-D50-S550 (c) R-D100-S225 (d) R-D100-S550	142
Figure 4.18	Backbone curves of retrofitted specimens (a) R-D50-S225 (b) R-D50-S550 (c) R-D100-S225 (d) R-D100-S550	144

Figure 4.19	Comparison among the stiffness degradation of retrofitted specimens (a) R-D50-S225 (b) R-D50-S550 (c) R-D100-S225 (d) R-D100-S550	147
Figure 4.20	Energy dissipation capacity of retrofitted specimens (a) R-D50-S225 (b) R-D50-S550 (c) R-D100-S225 (d) R-D100-S550	149
Figure 4.21	Measured strains of retrofitted specimens (a) Push direction (b) Pull direction	151
Figure 4.22	Measured strains of specimen R-D100-S225 (a) Strain ratio (web/flange) (b) strain in flanges	151
Figure 4.23	Comparison of failure modes of retrofitted and un-retrofitted specimens (a) R-D50-S225 (b) U-D50-S225 (c) R-D100-S225 (d) U-D100-S225	154
Figure 4.24	Comparison of failure modes of retrofitted and un-retrofitted specimens (a) R-D50-S550 (b) U-D50-S550 (c) R-D100-S550 (d) U-D100-S550	156
Figure 4.25	Comparison between the backbone curves of retrofitted and un-retrofitted specimens (a) D50-S225 (b) D50-S550 (c) D100-S225 (d) D100-S550	158
Figure 4.26	Comparison of stiffness degradation of retrofitted and un-retrofitted specimens (a) D50-S225 (b) D50-S550 (c) D100-S225 (d) D100-S550	161
Figure 4.27	Comparison of energy dissipation of retrofitted and un-retrofitted specimens (a) D50-S225 (b) D50-S550 (d) D100-S225 (c) D100-S550	163
Figure 4.28	Comparison of retrofitted and un-retrofitted specimens' measured strains (a) columns with chord distance of 50 mm (b) columns with chord distance of 100 mm	165
Figure 4.29	Comparison of R-D100-S225 and U-D100-S225 specimens' measured strains (a) Strain ratio (web/flange) (b) strain in flanges	166
Figure 5.1	Flow chart of numerical studies	170
Figure 5.2	Finite element model of the built-up battened columns in ABAQUS software (a) before meshing (b) after meshing	175
Figure 5.3	The C3D8I element used for simulation of columns (167)	176
Figure 5.4	Initial imperfection contours (a) local buckling (b) global buckling	179
Figure 5.5	Comparison of hysteresis loops	180

Figure 5.6	Comparison of the failure modes test vs. numerically predicted ones (a) D50-S225 (b) D100-S225 (c) D50-S550 (d) D100-S550	181
Figure 5.7	Effects of battens thickness on the failure modes of specimens (a) U-D50-S300-P10 (b) U-D50-S300-P20 (c) U-D50-S300-P40 (continue)	185
Figure 5.8	Effects of battens spacing and axial load on the failure modes of specimen (a) U-D50-S62-T5 (b) U-D50-S225-T5 (c) U-D50-S550-T5	187
Figure 5.9	Effects of chords distance on the failure modes of specimen (a) U-S300-T6-P10 (b) U-S300-T6-P20 (c) U-S300-T6-P40	188
Figure 5.10	Max. stress in battens along the height of columns (a) battens spacing 200 mm (b) battens spacing 300 mm (c) battens spacing 375 mm	190
Figure 5.11	The ratio of max. stress in chords to the max. stress in the batten measured at the base of columns (a) battens spacing 200 mm (b) battens spacing 300 mm (c) battens spacing 375 mm	191
Figure 5.12	Effect of battens thickness on the hysteresis loops of columns (a) U-D50-S200-P10 (b) U-D50-S200-P20 (c) U-D50-S200-P40	193
Figure 5.13	Comparison of the effect of battens thickness on the backbone curves of columns (a) U-D50-S200 (b) U-D50-300 (c) U-D50-S375	194
Figure 5.14	Effects of battens spacing on the hysteresis loops of columns (a) U-D50-P20-T4 (b) U-D50-P20-T6 (c) U-D50-P20-T8	196
Figure 5.15	Effect of battens spacing on the backbone curves of column (a) U-D50-T4 (b) U-D100-T4 (c) U-D150-T4	197
Figure 5.16	Effects of battens spacing on the hysteresis loops of columns (a) U-D50-P10-T6 (b) U-D50-P30-T6 (c) U-D50-P40-T6	199
Figure 5.17	Effect of battens spacing on the backbone curves of column (a) U-D50-T6 (b) U-D100-T6	200
Figure 5.18	Effect of batten spacing on the lateral load capacity of columns (a) chord distance of 50 mm (b) chord distance of 100 mm (c) chord distance of 150 mm	202
Figure 5.19	Effect of batten spacing on the lateral load capacity of columns (a) chord distance of 50 mm (b) chord distance of 100 mm	202

Figure 5.20	Comparison of design and FEA moments (a) 50 mm chord distance (b) 100 mm chord distance	202
Figure 5.21	Ductility ratio against the batten spacing (a) chord distance of 50 mm (b) chord distance of 100 mm (c) chord distance of 150 mm	204
Figure 5.22	Ductility ratio against the batten spacing (a) chord distance of 50 mm (b) chord distance of 100 mm	204
Figure 5.23	Effects of battens spacing on the energy dissipation capacity of columns (a) U-D50-T6-P10 (b) U-D100-T6-P10 (c) U-D150-T6-P10	207
Figure 5.24	Effects of battens spacing on the energy dissipation capacity of columns (a) U-D50-T6-P10 (b) U-D50-T6-P30 (c) U-D50-T6-P40	209
Figure 5.25	Effect of battens spacing on stiffness degradation of specimens (a) U-D50-P10-T5 (b) U-D50-P30-T5 (c) U-D50-P40-T5	210
Figure 5.26	Effect of chord distance on the hysteresis loops of columns (a) U-S200-T6-P10 (b) U-S200-T6-P20 (c) U-S200-T6-P40	212
Figure 5.27	Effect of chord distance on the backbone curves of columns (a) U-S200-T6 (b) U-S300-T6 (c) U-S375-T6	212
Figure 5.28	Effect of chord distances on the lateral load capacity of columns with (a) battens spacing 200 mm (b) battens spacing 300 mm (c) battens spacing 375 mm	214
Figure 5.29	Effect of chord distances on the ultimate lateral displacement of columns with (a) battens spacing 200 mm (b) battens spacing 300 mm (c) battens spacing 375 mm	214
Figure 5.30	Effect of chord distances on the ductility ratios of columns with (a) battens spacing 200 mm (b) battens spacing 300 mm (c) battens spacing 375 mm	215
Figure 5.31	Effects of chord distance on the energy dissipation capacity of columns (a) battens spacing 200 mm (b) battens spacing 300 mm (c) battens spacing 375 mm	217
Figure 5.32	Effect of chord distance on stiffness degradation of specimens (a) U-S200-P10-T6 (b) U-S200-P30-T6 (c) U-S200-P40-T6	219
Figure 5.33	Hysteresis loops of columns under different intensities of axial forces (a) U-D50-S62 (b) U-D50-S225 (c) U-D50-S550 (d) U-D50-S1200	220

Figure 5.34	Hysteresis loops of columns under different intensities of axial forces (a) U-D100-S62 (b) U-D100-S225 (c) U-D100-S550 (d) U-D100-S1200	221
Figure 5.35	Backbone curves of columns with the chord distance of 50 mm under different intensities of axial forces	222
Figure 5.36	Backbone curves of columns with the chord distance of 100 mm under different intensities of axial forces	222
Figure 5.37	Effect of axial load on the lateral load capacity of columns with (a) chord distance of 50 mm (b) chord distance of 100 mm (c) chord distance of 150 mm	224
Figure 5.38	Effect of axial load on the ultimate displacement of columns with (a) chord distance of 50 mm (b) chord distance of 100 mm (c) chord distance of 150 mm	224
Figure 5.39	Effect of axial load on the ductility ratio of columns with (a) chord distance of 50 mm (b) chord distance of 100 mm (c) chord distance of 150 mm	225
Figure 5.40	Comparison of the ratio of ultimate load to the effective yield strength of columns (a) chord distance of 50 mm (b) chord distance of 100 mm	226
Figure 5.41	Effects of axial load on the energy dissipation capacity of column D50 and (a) battens spacing 62 mm (b) battens spacing 225 mm (c) battens spacing 550 mm (d) battens spacing 1200 mm	229
Figure 5.42	Effect of axial load on stiffness degradation of specimens (a) U-D50-S62-T5 (b) U-D50-S225-T5 (c) U-D50-S550-T5 (d) U-D50-S1200-T5	231
Figure 5.43	Comparison of hysteresis loops of column R-D50-S550-P10	234
Figure 5.44	Comparison of the failure modes test vs. numerically predicted ones	235
Figure 5.45	Effect of CFRPs layers and axial load on the failure modes of retrofitted columns (a) R-D50-S225-1Pn-2L (b) R-D50-S225-1Pn-3L (c) R-D50-S225-1Pn-4L	237
Figure 5.46	Effect of number of retrofitted panels on the failure modes of columns (a) R-D50-S225-1Pn-2L (b) R-D50-S225-2Pn-2L	238
Figure 5.47	Effect of number of retrofitted panels on the failure modes of columns (a) R-D100-S225-1Pn-2L (b) R-D100-S225-2Pn-2L	239

Figure 5.48	Effect of retrofitted panels on the failure modes of columns (a) R-D50-S550-1Pn-2L (b) R-D100-S550-1Pn-2L	240
Figure 5.49	Effect of CFRP layers on the hysteresis loops of column (a) R-D50-S225-1Pn-2L (b) R-D50-S225-1Pn-3L (c) R-D50-S225-1Pn-4L	242
Figure 5.50	Effect of CFRP layers on the hysteresis loops of column (a) R-D50-S225-2Pn-2L (b) R-D50-S225-2Pn-3L (c) R-D50-S225-2Pn-4L	243
Figure 5.51	Effect of CFRP layers on the hysteresis loops of column (a) R-D50-S550-1Pn-2L (b) R-D100-S550-1Pn-2L	244
Figure 5.52	Effect of CFRP layers on the backbone curves of column (a) R-D50-S225-1Pn-2L (b) R-D50-S225-1Pn-3L (c) R-D50-S225-1Pn-4L	244
Figure 5.53	Effect of CFRP layers on the backbone curves of column (a) R-D50-S225-2Pn-2L (b) R-D50-S225-2Pn-3L (c) R-D50-S225-2Pn-4L	245
Figure 5.54	Effect of CFRP layers on the backbone curves of column (a) R-D50-S550-1Pn-2L (b) R-D100-S550-1Pn-2L	245
Figure 5.55	Effect of axial load and CFRPs layers on the ultimate strength of retrofitted columns (a) R-D50-S225-1Pn (b) R-D100-S225-1Pn (c) R-D50-S225-2Pn (d) R-D100-S225-2Pn	247
Figure 5.56	Effect of axial load and CFRPs layers on the ultimate strength of retrofitted columns (a) R-D50-S550-1Pn (b) R-D100-S550-1Pn	248
Figure 5.57	Effect of axial load and CFRPs layers on the displacement at ultimate load of retrofitted columns (a) R-D50-S225-1Pn (b) R-D100-S225-1Pn (c) R-D50-S225-2Pn (d) R-D100-S225-2Pn	251
Figure 5.58	Effect of axial load and CFRPs layers on the displacement at ultimate load of retrofitted columns (a) R-D50-S550-1Pn (b) R-D100-S550-1Pn	251
Figure 5.59	Effect of CFRPs layers and axial load on the ductility ratios of retrofitted columns (a) R-D50-S225-1Pn (b) R-D100-S225-1Pn	253
Figure 5.60	Effect of CFRPs layers and axial load on the ductility ratios of retrofitted columns (a) R-D50-S225-2Pn (b) R-D100-S225-2Pn	253

Figure 5.61	Effect of CFRPs layers and axial load on the ductility ratios of retrofitted columns (a) R-D50-S550-1Pn (b) R-D100-S550-1Pn	254
Figure 5.62	Effect of CFRPs layers and axial load on energy dissipation capacity of columns (a) R-D50-S225-1Pn-P10 (b) R-D50-S225-1Pn-P30 (c) R-D50-S225-1Pn-P40	257
Figure 5.63	Effect of CFRPs layers and axial load on energy dissipation capacity of columns (a) R-D50-S225-2Pn-P10 (b) R-D50-S225-2Pn-P30 (c) R-D50-S225-2Pn-P40	258
Figure 5.64	Effect of CFRPs layers and axial load on energy dissipation capacity of columns (a) R-D50-S550-1Pn-2L (b) R-D100-S550-1Pn-2L	259
Figure 5.65	Effect of CFRPs layers and axial load on stiffness degradation of columns (a) R-D50-S225-1Pn-P10 (b) R-D50-S225-1Pn-P30 (c) R-D50-S225-1Pn-P40	262
Figure 5.66	Effect of CFRPs layers and axial load on stiffness degradation of columns (a) R-D50-S225-2Pn-P10 (b) R-D50-S225-2Pn-P30 (c) R-D50-S225-2Pn-P40	264
Figure 5.67	Effect of CFRPs layers and axial load on stiffness degradation of columns (a) R-D50-S550-1Pn-2L (b) R-D100-S550-1Pn-2L	265

LIST OF ABBREVIATIONS

AISC	-	American society of steel construction
AFRP	-	Aramid fibre reinforced polymer
ASTM	-	American society of testing of materials
CCFT	-	Circular concrete filled tubes
CFDST	-	Concrete-filled double skin steel tubular
CFS	-	Cold formed steel
CCFST	-	Curved concrete-filled steel tubular trusses
CFST	-	Concrete filled steel tubes
CFRP	-	Carbon fibre reinforced polymer
DCBB	-	Double channel back-to-back
DCFF	-	Double channel face-to-face
DI	-	Double I-sections
EC3	-	Eurocode 3
FEM	-	Finite element method
FRP	-	Fibre reinforced polymer
GFRP	-	Glass fibre reinforced polymer
HRS	-	Hot rolled steel
HSS	-	Hollow structural sections
LTB	-	Lateral torsional buckling
LVDT	-	Linear Variable Differential Transforms
RA	-	Recycled aggregate
RACFT	-	Recycled aggregate concrete filled tube
RC	-	Reinforced concrete
SHS	-	Square hollow sections
SCFST	-	Square concrete filled steel tubes

LIST OF SYMBOLS

A_{ch}	-	Sectional area of chord
A_g	-	Gross cross-sectional area
d	-	Distance between the chords
E	-	Modulus of elasticity
e_o		Bow imperfection
F_y	-	Yield strength
F_u	-	Ultimate strength
F_{cr}	-	Critical buckling stress
F_e	-	Elastic buckling stress
h_o	-	Distance between the centroid of Chords
h	-	Web height
I_{eff}	-	Effective moment of inertia
K_m	-	Effective length factor
M	-	Bending moment
M_{Ed}	-	Design value of the maximum moment
M_{pce}	-	Plastic moment capacities
N_{cr}	-	Effective critical force
N_{Ed}	-	Design value of the compression force
P_n	-	Nominal strength
P	-	Axial load
P_{ye}	-	Expected axial yield capacity
R	-	Retrofitted
R_y	-	Ratio of the expected yield stress to the specified minimum yield stress
r	-	Radius of Gyration
r_i	-	minimum radius of gyration
s	-	Centre to centre spacing of battens
S_v	-	Shear stiffness
SG	-	Strain gauge
t_f	-	Flange thickness

t_w	-	Web thickness
μ	-	Ductility ratio
U	-	Un-retrofitted
V	-	Shear force
ν	-	Poisson ratio
w	-	Flange width
δ_u	-	Ultimate displacement
δ_y	-	Yield displacement

LIST OF APPENDICES

APPENDIX	TITLE	PAGE
Appendix A	Design procedure of moment resisting frame	293
Appendix B	Failure modes of un-retrofitted columns	300
Appendix C	Effect of battens thickness on the cyclic response of un-retrofitted columns	304
Appendix D	Effect of battens spacing on the cyclic response of un-retrofitted columns	305
Appendix E	Effect of axial force on the cyclic response of un-retrofitted columns	310
Appendix F	Effect of the retrofitted panel, CFRPs layers and axial force on the cyclic response of columns	313

CHAPTER 1

INTRODUCTION

With the existence of life, human beings have always been in search of a safe shelter for their living and safety, for that in the start; they used stones, wood, mud etc., to build a safe place. By the time they started improving their living standard by inventing new construction techniques and materials such as bricks, cement, steel etc. Steel has been used in the construction industry on a vast scale due to its higher strength, durability and ease of fabrication and erection compared to other materials. It is used in constructing high-rise buildings (skyscrapers) and longer span bridges as framed structures almost worldwide. But at the same time, the failure of these structures caused the loss of human life and economy, which may be attributed to the lack of proper design rules, poor quality of material, defective workmanship or a natural disaster such as floods, tsunami or occurrences of frequent Earthquakes.

Among natural disasters, earthquakes have been one of the leading causes of human casualties and property destruction. It is reported that there have been 1.87 million deaths due to earthquakes in the 20th century (1). As a catastrophic event, Earthquake has always been the main concern for civil engineers, despite knowing that we can't eliminate earthquake disasters but with a struggle to save human life as much as possible. Earthquakes may cause structural and non-structural damage during seismic excitations. Structural damages consist of distress induced in structural components of lateral and gravity-load-resisting systems, such as beams, columns, load-bearing walls, and shear walls, as well as horizontal diaphragms, such as slabs and roofs.

There's a saying among seismologists: "Earthquakes don't kill people, Buildings kill people."

Which is true, because seismic damage in structures is caused either by underestimating or avoiding the seismic forces or lack of sufficient strength or lack of inelastic deformability. Lack of strength and/or deformability creates seismically deficient structures that often suffer significant damage during strong earthquakes. Under all such conditions, damage occurs at the critical regions of structures. Properly designed and detailed structures tend to perform in a ductile manner and dissipate seismic-induced energy, reducing vulnerability against earthquake damage, such as columns, which are often responsible for the overall strength and stability of the entire structural system.

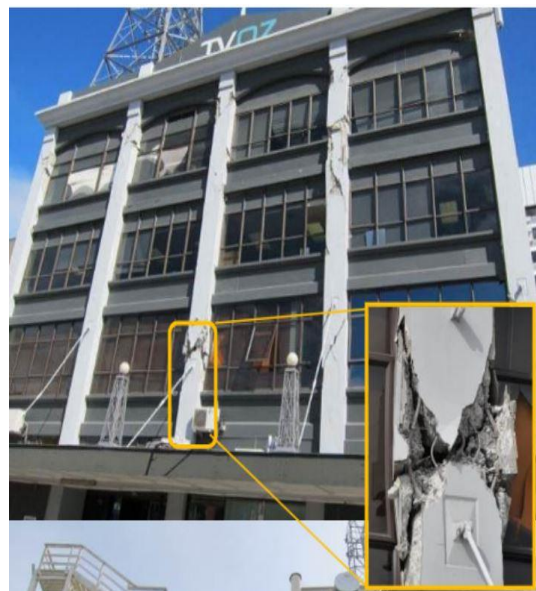
The role of columns in the structures is like a backbone in the human body because the stability of the whole structure is dependent on the performance of columns. It is the part of the structure subjected to almost all loadings such as compression, bending, torsion and shear; losing one column can result in partial or complete structural collapse. That is the reason that most of the design standards have introduced the strong column-weak beam concept to ensure that the seismic energy is dissipated through beams and girders rather than the columns. But despite such guidelines, the formation of plastic hinges in columns during a severe earthquake is still unavoidable. The ability of the structure to withstand against earthquakes and to perform adequately in the inelastic range highly depends on the formation of these plastic hinges and their capability to absorb and distribute the seismic energy. Therefore, column performance in the inelastic mode is of utmost importance for the safety of a structure during an earthquake.

Low seismic resistance of columns is the most likely cause for structures collapse during earthquakes, resulting in significant human and economic loss. The importance of columns can be clearly understood from the damages that occurred in the various structures due to column failures during past earthquakes, as shown in Figure 1.1. Earthquake in Turkey happened on May 1, 2003, at Bingol (see Figure 1.1(a)) resulted in the collapse of many buildings (2), the Canterbury Television

building (see Figure 1.1(b)) in Christchurch, New Zealand, fell after the 2011 Christchurch earthquake killing 115 people due to insufficient seismic design and structural ductility (3). Similarly, the failure of bridge columns in the 1995 Kobe Earthquake and Loma Prieta 1989 earthquake (see Figure 1.1(c-d)) also caused huge loss of life and economy.



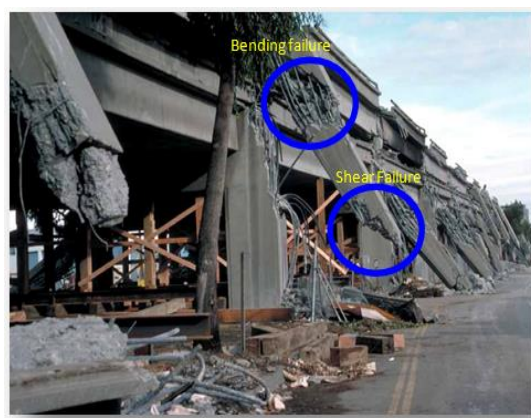
(a) Diagonal tension failure in columns, in an Earthquake in Turkey (2)



(b) Shear failure of a column, Christchurch earthquake in New Zealand (3)



(c) Flexural and Shear failure of an expressway columns 1995 Kobe earthquake (4)



(d) Failure of Cypress viaduct columns Loma prieta 1989 (5)



(e) Building Column Hinging at Base and Top (6)



(f) Collapse of Buildings due to Strong Beam-weak Columns (6)(7)



(g) Lack of confinement reinforcement (6)

(h) Shear failure of Bridge Columns (6)

Figure 1.1 Column failure modes

Built-up columns are usually adopted when the single rolled section can't fulfil the desired requirements such as higher axial strength, the moment of inertia, excessive bending and torsional resistance etc. The individual rolled steel sections such as I-sections and C-sections have a larger moment of inertia along the axis perpendicular to the web of sections called the strong axis of sections. The axis parallel to the web is the weak axis of the section. Therefore, the buckling strength of the individual sections is high in the plane of the web and weak in the opposite axis. The 'Built-up' section is used to counter such geometrical deficiency of the individual rolled sections. Built-up columns consist of two or more longitudinal sections which are interconnected by transverse members, which hold them to form an integral unit with a continuous longitudinal space between the sections. Depending on the way of connections between the flanges of the sections and the method of force transfer, they are categorised as built-up battened columns and built-up laced columns, as shown in Figure 1.2. These transverse members, such as battens (frame action) or lacing bars (truss action), also act as the shear connection between the longitudinal members to resist the shearing forces. In addition, these transverse connections are also used to reduce the effective length of the main members between the points of transverse connections to prolong the local buckling such that it doesn't occur before the global one. Steel plates or angles are usually used to fabricate battens or laced members. The longitudinal sections of built-up columns are called chords and often made by channel or I-shaped profiles. These longitudinal sections of built-up columns can be of different cross sections and arrangements, as shown in Figure 1.3. The built-up columns mostly failed due to the local buckling of flanges and web of the main chord at the lower panel irrespective of the section's types and arrangements as shown in Figure 1.3. However, the columns composed of I-sections as chord members showed higher lateral strength and potential to reach the M_p of the sections than columns with composed of channel sections (8)(9)(10). Therefore, it is of great interest to determine the governing failure mode of built-up battened columns composed of channels sections considering the effects of batten thickness and spacing, chord distance, and axial force. In addition, an efficient strengthening method is also necessary to counter such excepted failures in built-up battened columns during seismic events.

Similarly, the steel structures are also vulnerable to seismic excitation, as observed during past earthquakes in Bam in December 2003 in Iran, with a loss of 35000 precious life (11)(12)(13). Where the most of the residential and commercial steel buildings constructed using built-up columns were seriously damaged. As a result, different failure modes were observed in the built-up columns, as shown in Figure 1.4. The observed failure mechanisms of built-up columns highlight uncertainties regarding these columns' seismic behaviour.

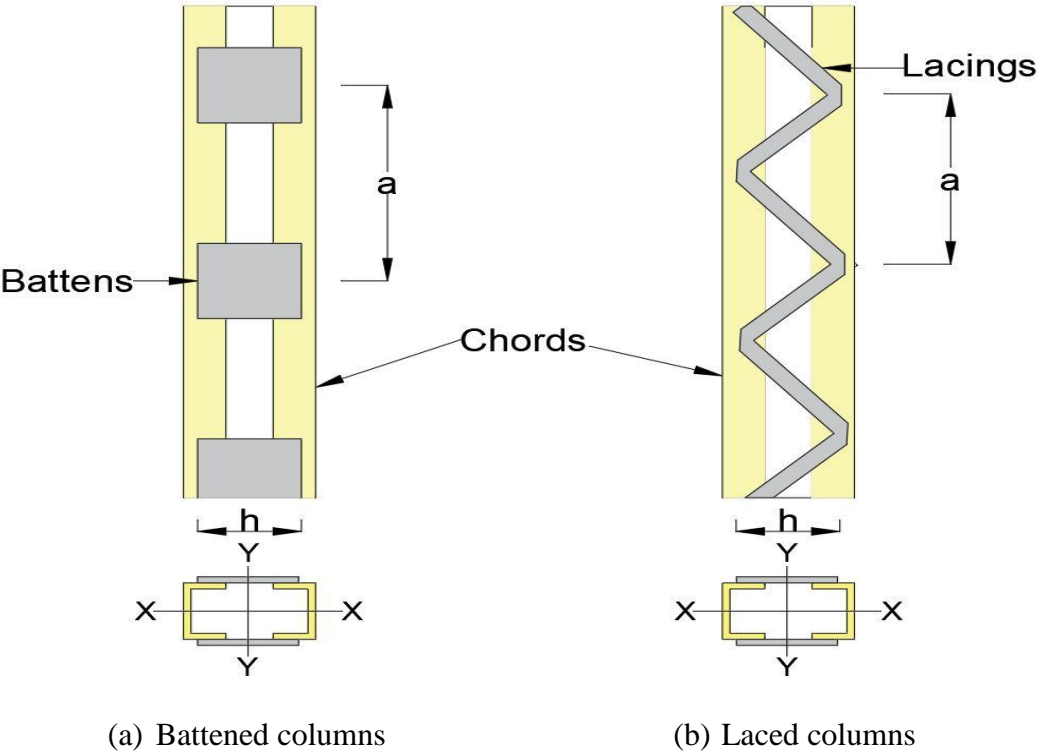


Figure 1.2 Types of built-up (a) battered columns (b) laced columns

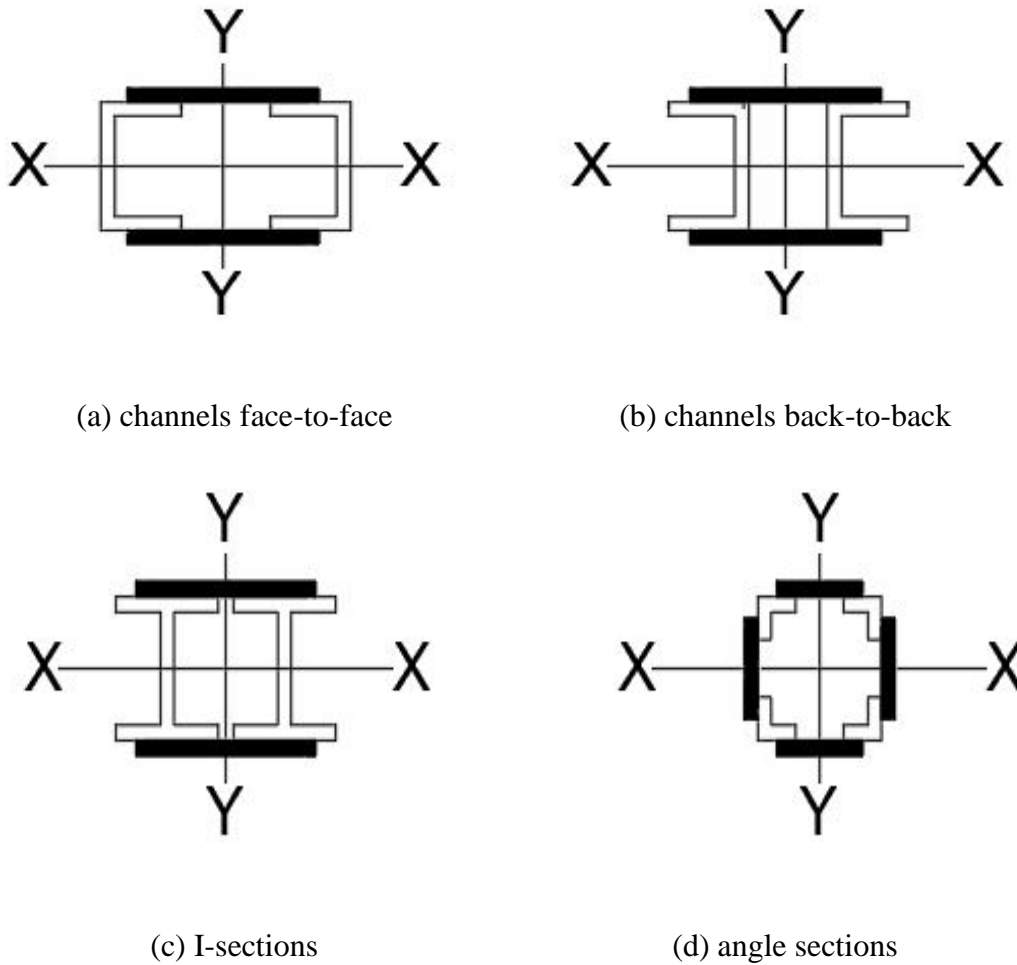


Figure 1.3 Types of built-up sections (a) channels face-to-face (b) channels back-to-back (c) I-sections (d) angle section (continue)

1.1 Problem Statement

Columns play a significant role in the stability of structures under gravity and lateral loads. Failure of a column can result in partial or complete collapse of a building. From the history of the past earthquakes, it was found that the built-up battened columns are seismically vulnerable. As shown in Figure 1.4, different types of failure mode, such as plastic deformation of battens, fracture of battens, global buckling of columns, local buckling of web and flanges and formation of plastic hinges at the bottom of built-up columns have been observed for these columns (11,12). Therefore, it is of great interest to determine the governing failure mode of

these columns considering the effects of batten thickness and spacing, chord distance, and axial force.



Plastic deformation of battens



Fracture of battens



Global buckling of columns



Local buckling of column

Figure 1.4 Failure modes of built-up battened columns (11)

Besides, most of the design codes (14–16) do not provide any seismic design specifications for built-up battened columns; consequently, structural design of these columns has been based on equations given for gravity loads. This implies that further investigations are needed to explore the bending capacity, stiffness degradation rate, ductility ratio, and energy dissipation capacity of built-up columns designed in accordance with current design codes. The outcome of such investigations is also important for the seismic analysis of built-up columns. This is mainly due to the fact that so far it is not known these columns should be classified

as force-controlled or deformation-controlled, based on the requirements of ASCE 41-17 (17).

Considering the fact that these columns have often suffered significant damage during past earthquakes, it is also necessary to propose an efficient strengthening method for them that is practical in use by design engineers. It is worth mentioning that still there is no practical method for retrofitting of built-up battened columns against seismic actions. Previous retrofitting strategies have mostly focused on solid/hollow sections (18)(19)(20)(21)(22)(23).

1.2 Research Objectives

The overall focus of this study is to gain a profound insight into the seismic performance of built-up battened columns by considering the various parameters and developing a retrofitting technique. Followings are specific objectives:

- (a) To determine the governing failure mode of built-up battened columns under quasi-static cyclic load through experimental works and numerical simulations.
- (b) To determine the effect of batten's thickness, batten spacing, and chord distance on the ultimate load, ductility ratio, and energy dissipation capacity of built-up battened columns through experimental works and numerical simulations.
- (c) To investigate the effect of axial force on the ultimate load, ductility ratio, and energy dissipation capacity of built-up battened columns through numerical simulations.
- (d) To propose a strengthening method for deficient built-up battened columns and examine its efficiency through experimental works and numerical simulations.

1.3 Scope of the study

This study will only concentrate on the built-up battened columns composed of two plain channel sections. The channels will be placed face to face at different distances (i.e., 50 mm, 100 mm and 150 mm) and will be attached through welding with the help of battens with different spacings (i.e., 62 mm, 200 mm, 225 mm, 300 mm, 375 mm, 550 mm and 1200 mm) and thicknesses (i.e., 4 mm, 6 mm and 8 mm). Mild steel channel sections will be used with the yield and ultimate strength of 373 and 508 MPa, respectively. The yield and ultimate strength of the batten's plates will be 388 and 568 MPa, respectively. The column will be subjected to a constant axial force of 10%, 20%, 30% and 40% of their yield load and quasi-static cyclic loading, using FEMA 461 for load protocol. Bending will be considered only around the material free axis of the column. For retrofitting of the section's Sika Grout with the seven days, compressive strength of 25 MPa will be used as infill material, and carbon fibre reinforced polymer (CFRP) used had an elastic modulus of 252 GPa, the ultimate tensile strength of 4900 MPa and an ultimate strain of 2% based on a nominal thickness of 0.164 mm per ply, for external wrapping. This study will be limited to investigating the application of CFRP material only as an external reinforcement, and unidirectional CFRP sheets will be used in this research. Only the lateral effect of the CFRP strengthening technique will be covered in this study; the axial response of the retrofitted section will not be considered. Long term behaviour and environmental impacts of CFRP will also not be covered here.

1.4 Significance of the study

It has been shown during past earthquakes that built-up battened columns have been vulnerable against seismic actions. One main reason to these observations is that seismic design codes do not provide any specifies seismic design guideline for these columns. The outcome of this study will significantly enhance our understanding about the governing failure mode of built-up columns. Besides, since the effect of batten thickness, batten spacing, chord distance and axial force on the seismic behavior of these columns will be investigated, this study can help to prepare

a specific seismic design guidelines for built-up columns. Furthermore, since this study proposes an efficient retrofitting method for the existing built-up columns that are vulnerable against seismic actions, it can enhance the safety of buildings.

1.5 Layout of Thesis

The composition of the thesis is organized into six chapters. Chapter 1 provides background information on the needs and objectives of the current study. Chapters two to six present the literature review, methodology used in the current study, experimental and theoretical studies, numerical study on various aspects and end conclusion of the current research, respectively. Meanwhile, a series of key findings and critical conclusions are summarized at the end of each chapter. Details of these chapters are outlined below.

Chapter 2 presents a review of the existing literature covering topics related to the present study. First, a brief introduction of built-up battened columns is provided, followed by a broad review of its design guide lines in various codes are discussed. These are followed by a review on the shortcomings of the built-up battened columns, with particular attention to the slenderness ratio, shear effect, compound buckling, axial performance and sectional slenderness ratio of the sections on their axial and cyclic performance. Then some previous studies on the cyclic response of built-up battened and laced columns are provided. The static and cyclic behaviour of retrofitted sections such as CFST sections and the sections strengthened with CFRP are then reviewed and compared to highlight the advantages of CFST sections and CFRP wrapping.

Chapter 3 shows the methodology of experimental work used in the current research program for the testing of four conventional hollow sections and four retrofitted built-up battened sections. This study consists of four objectives based on experimental work and numerical simulation. As shown in Figure 1.5, the first, second and fourth objectives involved experimental work and numerical simulation, while the third objective was only based on numerical simulation. The initial step in

the experimental procedure was to identify the quantity and size of test specimens for each objective based on the limitations imposed by laboratory equipment. A total of eight specimens were designed and constructed in a workshop. After the construction of specimens, the next step was to design the test setup and determine the appropriate instrumentation plan for the acquisition of data. Finally, the test specimens were loaded one by one in accordance with the research objectives, and the data was collected for comparison and discussion. Material tests that include tests on the steel, grout and CFRP were also performed to find out the mechanical properties of the employed material.

Chapter 4 first presents the experimental results of four conventional samples tested in the laboratory with different battens spacing and chords distance. Then the results of four retrofitted sections are provided. In both cases, the failure modes of the tested samples were discussed in detail. Next, the performance of all the tested samples was judged in terms of hysteresis loops, backbone curves, stiffness degradation, energy dissipation, strain measurement, displacement ductility ratio, initial and post-yield stiffness. In the end, a comparative study was done between the conventional and retrofitted sections.

Chapter 5 reports the results of numerical analysis obtained using ABAQUS software in the current study. As shown in Figure 1.5, all the four objectives of the current study involve numerical simulation. The first step in the numerical simulation was modelling the parts of the specimen. After modelling, the second step was assigning material properties to each part of the specimen. In the third step, the parts were assembled to form a single specimen, and the interaction between the parts was assigned. The fourth step was the application of loading protocols, boundary conditions and analysis type. The fifth and last step was meshing each part of the specimen. After analysis, the numerical results were validated with the experimental ones. After validation, the parametric study for each objective was conducted, and the data was collected for further analysis and comparison.

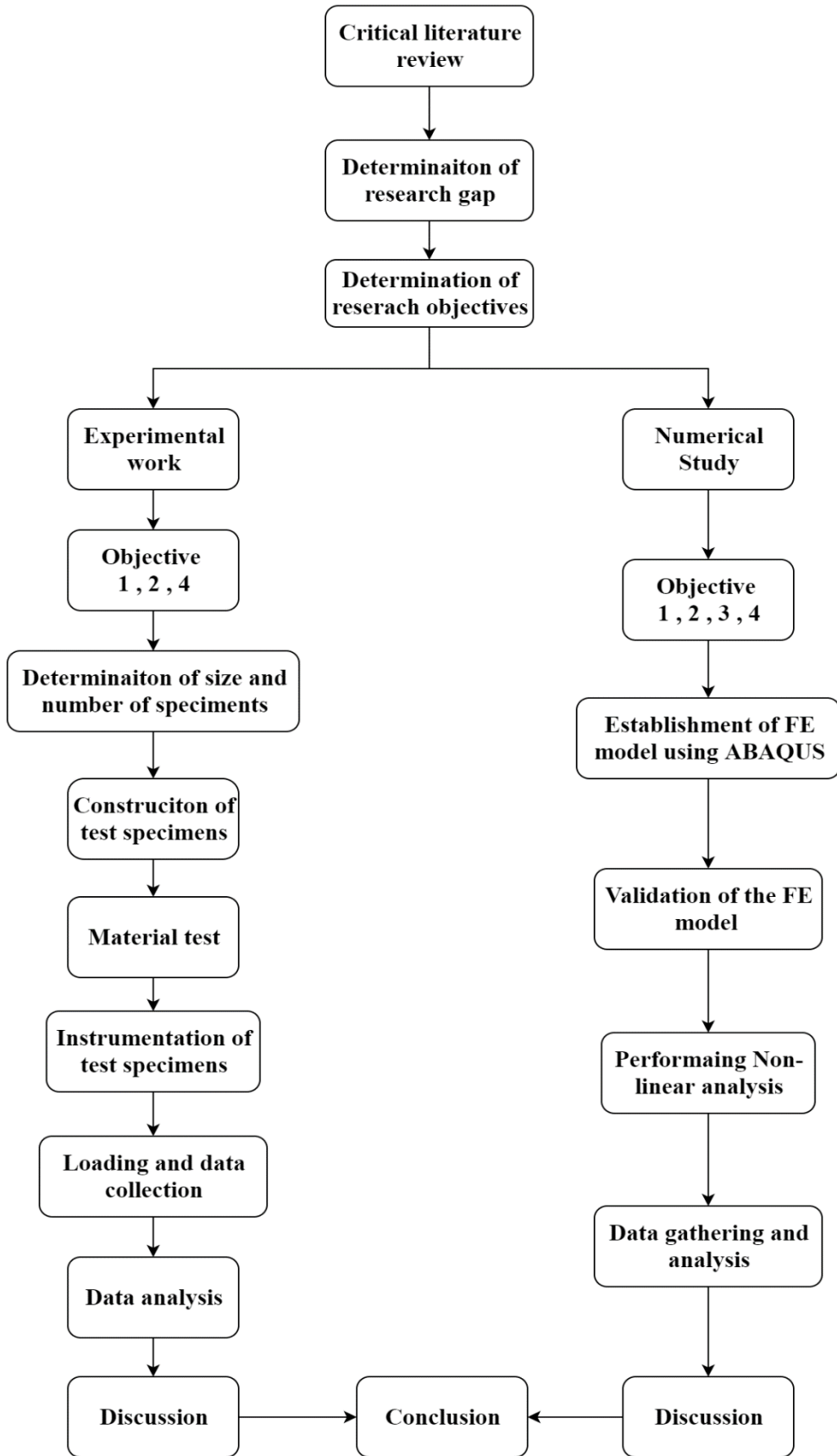


Figure 1.5 Research methodology flow chart

Chapter 6 finally compares and summarizes the findings of this study from experimental work and numerical simulation and highlights the significance of the research project. Suggestions and recommendations for future investigation will be presented.

REFERENCES

1. Guha-Sapir D, Below R, Hoyois P. EM-DAT: International disaster database. Cathol Univ Louvain Brussels, Belgium. 2015;27(2015):57–8.
2. Isler O. Seismic Performances and Typical Damages of Beam-Column Joints in the RC Buildings. 14th World Conf Earthq Eng. 2008;(2007).
3. Kam, W. Y., Pampanin, S., & Elwood K. Seismic Performance of Reinforced Concrete Buildings in the 22February Christchurch (Lyttel Ton) Earthquake. Bull New Zeal Soc Earthq Eng. 2011;44:239–78.
4. Anderson DL, Mitchell D, Tinawi RG. Performance of concrete bridges during the Hyogo-ken Nanbu (Kobe) earthquake on January 17, 1995. Can J Civ Eng. 1996;23(3):714–26.
5. Zhiqiang W, Lee GC. A comparative study of bridge damage due to the Wenchuan, Northridge, Loma Prieta and San Fernando earthquakes. Earthq Eng Eng Vib. 2009;8(2):251–61.
6. Murat Saatcioglu. Structural Damage Caused by Earthquakes. University of Ottawa, Ottawa, ON, Canada Definitions. 2013. 941–947 p.
7. Doğangün A, Ural A, Sezen H, Güney Y, Fırat F. The 2011 Earthquake in Simav, Turkey and Seismic Damage to Reinforced Concrete Buildings. Buildings. 2013;3(1):173–90.
8. Sahoo DR, Rai DC. Built-up battened columns under lateral cyclic loading. Thin-Walled Struct. 2007;45(5):552–62.
9. Sahoo D, Rai DC. Battened Built-Up Beam-Columns Under Cyclic Loads. 13th World Conf Earthq Eng. 2004;(67).
10. Sarkar S, Sahoo DR. Effect of chord configuration and spacing on cyclic flexural response of built-up columns. Int J Steel Struct. 2016 Jun 30;16(2):441–53.
11. Hashemi BH, Jafari S. M. Performance of Batten Columns in Steel Buildings During the Bam Earthquake of 26 December 2003. Struct Eng Res Center, Int Inst Earthq Eng Seismol (IIEES),. 2004;101–9.
12. Hosseinzadeh NA. Lessons Learned from Steel Braced Buildings Damaged by the Bam Earthquake of 26 December 2003. Underw Technol [Internet].

- 2004;(September):11–3. Available from:
<http://jsee.ir/index.php/jsee/article/view/59>
13. S.M. Zahrai and M. Heidarzadeh. Destructive Effects of the 2003 Bam Earthquake on Structures. *Asian J Civ Eng (Building Housing)*. 2007;8(3):329–42.
 14. ANSI/AISC 360-16. Specification for Structural Steel Buildings ANSI/AISC 360-16. Aisc. 2016. 676 p.
 15. European committee For Standardisation. EN 1993-1-1: Eurocode 3: Design of steel structures - Part 1-1: General rules and rules for buildings. 2005.
 16. Bureau of Indian Standard. General construction in steel: Code of Practice. 3rd Revision. Bur Indian Stand New Delhi, India,. 2007;(IS800-2007).
 17. ASCE/SEI 41-17. Seismic Evaluation and Retrofit of Existing Buildings [Internet]. ASCE. Reston, VA: American Society of Civil Engineers; 2017. Available from: <http://ascelibrary.org/doi/book/10.1061/9780784414859>
 18. Lai M, Li C, Ho JCM, Chen MT. Experimental investigation on hollow-steel-tube columns with external confinements. *J Constr Steel Res* [Internet]. 2020;166:105865. Available from: <https://doi.org/10.1016/j.jcsr.2019.105865>
 19. Han LH, Huang H, Tao Z, Zhao XL. Concrete-filled double skin steel tubular (CFDST) beam-columns subjected to cyclic bending. *Eng Struct*. 2006;28(12):1698–714.
 20. Yoshiaki Goto MATE and XL. Local Buckling Restraining Behavior of Thin-Walled Circular CFT Columns under Seismic Loads. *J Struct Eng*. 2014;1(June):1–14.
 21. Ekiz E, El-tawil S, Parra-montesinos G, Goel S. Enhancing Plastic Hinge Behavior in Steel Flexural Members Using Cfrp Wraps. 2004;(2496).
 22. El-Tawil S, Ekiz E, Goel S, Chao SH. Retraining local and global buckling behavior of steel plastic hinges using CFRP. *J Constr Steel Res* [Internet]. 2011;67(3):261–9. Available from:
<http://dx.doi.org/10.1016/j.jcsr.2010.11.007>
 23. Tafsirojjaman T, Fawzia S, Thambiratnam DP, Wirth N. Performance of FRP strengthened full-scale simply-supported circular hollow steel members under monotonic and large-displacement cyclic loading. *Eng Struct* [Internet]. 2021;242(May):112522. Available from:
<https://doi.org/10.1016/j.engstruct.2021.112522>

24. Sahoo DR, Rai DC. Design and evaluation of seismic strengthening techniques for reinforced concrete frames with soft ground story. *Eng Struct* [Internet]. 2013;56:1933–44. Available from: <http://dx.doi.org/10.1016/j.engstruct.2013.08.018>
25. Montuori R, Piluso V. Reinforced concrete columns strengthened with angles and battens subjected to eccentric load. *Eng Struct* [Internet]. 2009;31(2):539–50. Available from: <http://dx.doi.org/10.1016/j.engstruct.2008.10.005>
26. Coletti D, Puckett J, Incorporated HDRE, Administration FH. *Steel Bridge Design Handbook: Structural Behavior of Steel*. 2012.
27. RONALD D. ZIEMIAN. *Guide to Stability Design Criteria for Metal Structures* [Internet]. Ziemian RD, editor. JOHN WILEY & SONS, INC. Hoboken, NJ, USA: John Wiley & Sons, Inc.; 2010. Available from: <http://doi.wiley.com/10.1002/9780470549087>
28. Aslani F, Goel SC. Stitch Spacing and Local Buckling in Seismic-Resistant Double-Angle Braces. *J Struct Eng*. 1991 Aug;117(8):2442–63.
29. Reyes-Salazar A, Bojórquez E, Bojorquez J, Valenzuela-Beltran F, Llanes-Tizoc MD. Energy Dissipation and Local, Story, and Global Ductility Reduction Factors in Steel Frames under Vibrations Produced by Earthquakes. *Shock Vib*. 2018;2018:1–19.
30. European Standard. EN 1998-1, Design of structures for earthquake resistance. 2004.
31. Mazzolani G. *Ductility Of Seismic Resistant Steel Structures*. USA: Taylor and Francis Ltd.; 2002. 360 p.
32. Gioncu V. Framed structures. Ductility and seismic response: General Report. *J Constr Steel Res*. 2000;55(1–3):125–54.
33. Wang YB, Li GQ, Cui W, Chen SW. Seismic behavior of high strength steel welded beam-column members. *J Constr Steel Res* [Internet]. 2014;102:245–55. Available from: <http://dx.doi.org/10.1016/j.jcsr.2014.07.015>
34. Park R. Ductility evaluation from laboratory and analytical testing [Internet]. *Proceedings of the 9th World Conference on Earthquake Engineering*, 2-9 August. 1988. p. 605–16. Available from: http://www.iitk.ac.in/nicee/wcee/article/9_vol8_605.pdf
35. Bleich F. *Buckling Strength of Metal Structures*. New York: McGraw-Hill;

1952. 503 p.
36. Stephen P. Timoshenko JMG. Theory of elastic stability. New York: McGraw-Hill,; 1961. 280 p.
 37. AISC 360-10. Specification for Structural Steel Buildings. Ansi/Aisc 360-10. 2010;
 38. Duan L, Chen W. Design Rules of Built-Up Members in Load and Resistance Factor Design. J Struct Eng. 1988 Nov;114(11):2544–54.
 39. Temple MC, Elmahdy G. Equivalent slenderness ratio for built-up members. Can J Civ Eng. 1993;20(4):708–11.
 40. Temple C, Temple MC, Elmahdy G, Temple C. Buckling of built-up compression members in the plane of the connectors. Can J Civ Eng. 1993;20(6):895–909.
 41. Temple MC, Elmahdy G. Local effective length factor in the equivalent slenderness ratio. Can J Civ Eng. 1995;22(6):1164–70.
 42. Temple MC, Elmahdy GM. Slenderness ratio of main members between interconnectors of built-up compression members. Can J Civ Eng. 1996;23(6):1295–304.
 43. Lue DM, Yen T, Liu J-L. Experimental investigation on built-up columns. J Constr Steel Res [Internet]. 2006 Dec;62(12):1325–32. Available from: <https://linkinghub.elsevier.com/retrieve/pii/S0143974X06000368>
 44. Liu J-L, Lue DM, Lin CH. Investigation on slenderness ratios of built-up compression members. J Constr Steel Res [Internet]. 2009 Jan [cited 2020 Mar 15];65(1):237–48. Available from: <https://linkinghub.elsevier.com/retrieve/pii/S0143974X08000692>
 45. Hosseini Hashemi B, Jafari MA. Experimental evaluation of elastic critical load in batten columns. J Constr Steel Res [Internet]. 2009;65(1):125–31. Available from: <http://dx.doi.org/10.1016/j.jcsr.2008.02.016>
 46. A. G. Razdolsky. Determination of Slenderness Ratio for Laced and Battened Columns. Pract Period Struct Des Constr. 2018;23(4):1–11.
 47. ASD A. Specification for Structural Steel Buildings. 1989;210.
 48. Duan L, Reno M, Uang CM. Effect of compound buckling on compression strength of built-up members. Eng J. 2002;39(1):30–7.
 49. AISC. Manual of Steel Construction, Load and Resistance Factor Design. Am Inst Steel Constr. 1999;(Suite 3100 Chicago, IL 60601).

50. Kalochairetis KE, Gantes CJ. Numerical and analytical investigation of collapse loads of laced built-up columns. *Comput Struct* [Internet]. 2011 Jun;89(11–12):1166–76. Available from: <https://linkinghub.elsevier.com/retrieve/pii/S0045794910002506>
51. Li Y, Cheng W, Wang B, Ren Y. Investigation on elastic compound buckling of latticed columns considering eccentricity and geometric imperfections. *Adv Mech Eng*. 2019;11(5):1–17.
52. AISC 341-16. Seismic Provisions for Structural Steel Buildings, ANSI/AISC 341-10. In: *Structural Analysis and Design of Tall Buildings*. CRC Press; 2011. p. 355–410.
53. Kurata M, Nakashima M, Suita K. Effect of column base behaviour on the seismic response of steel moment frames. *J Earthq Eng*. 2005;9(SPEC. ISS. 2):415–38.
54. El Aghoury MA, Salem AH, Hanna MT, Amoush EA. Experimental investigation for the behaviour of battened beam-columns composed of four equal slender angles. *Thin-Walled Struct* [Internet]. 2010 Sep;48(9):669–83. Available from: <https://linkinghub.elsevier.com/retrieve/pii/S0263823110000534>
55. El Aghoury MA, Salem AH, Hanna MT, Amoush EA. Ultimate capacity of battened columns composed of four equal slender angles. *Thin-Walled Struct* [Internet]. 2013 Feb;63:175–85. Available from: <https://linkinghub.elsevier.com/retrieve/pii/S0263823112002042>
56. El Aghoury MA, Salem AH, Hanna MT, Amoush EA. Strength of cold formed battened columns subjected to eccentric axial compressive force. *J Constr Steel Res*. 2015;113:58–70.
57. Astaneh-Asl A, Goel SC. Cyclic In-Plane Buckling of Double Angle Bracing. Vol. 110, *Journal of Structural Engineering*. 1984. p. 2036–55.
58. Suzuki Y, Lignos D. Collapse Behavior of Steel Columns as Part of Steel Frame Buildings: Experiments and Numerical Models. 16th World Conf Earthq Eng (16WCEE), January 9-13. 2017;Paper N° 1032.
59. Chou CC, Chen GW. Lateral cyclic testing and backbone curve development of high-strength steel built-up box columns under axial compression. *Eng Struct*. 2020;223(August):111147.
60. Standard AIJD, Structures S, Concept AS. AIJ Design Standard for Steel

- Structures Based on Allowable Stress Concept — (2005 Edition)
Architectural Institute of Japan. 2017;
61. Moghaddam H, Sadrara A, Jalali SR. Seismic performance of stainless-steel built-up box columns subjected to constant axial loads and cyclic lateral deformations. *Structures* [Internet]. 2021;33(February):4080–95. Available from: <https://doi.org/10.1016/j.istruc.2021.07.014>
 62. Dar MA, Sahoo DR, Jain AK. Influence of chord compactness and slenderness on axial compression behavior of built-up battened CFS columns. *J Build Eng* [Internet]. 2020;32(August):101743. Available from: <https://doi.org/10.1016/j.jobe.2020.101743>
 63. Fadden M, McCormick J. Cyclic Quasi-Static Testing of Hollow Structural Section Beam Members. *J Struct Eng*. 2012;138(5):561–70.
 64. Dabaon M, Ellobody E, Ramzy K. Experimental investigation of built-up cold-formed steel section battened columns. *Thin-Walled Struct* [Internet]. 2015;92:137–45. Available from: <http://dx.doi.org/10.1016/j.tws.2015.03.001>
 65. Dabaon M, Ellobody E, Ramzy K. Nonlinear behaviour of built-up cold-formed steel section battened columns. *J Constr Steel Res* [Internet]. 2015;110:16–28. Available from: <http://dx.doi.org/10.1016/j.jcsr.2015.03.007>
 66. AISI-S100-2007. North American Specification for the Design of Cold-Formed Steel Structural Members. *Aisi S100-2007*. 2007;
 67. Vijayanand S, Anbarasu M. Strength and behavior of cold-formed steel built-up battened columns : tests and numerical validation. 2019;46(2):154–64.
 68. Roy K, Mohammadjani C, Lim JBP. Experimental and numerical investigation into the behaviour of face-to-face built-up cold-formed steel channel sections under compression. *Thin-Walled Struct*. 2019;134:291–309.
 69. Roy K, Lim JBP. Numerical investigation into the buckling behaviour of face-to-face built-up cold-formed stainless steel channel sections under axial compression. *Structures*. 2019;20:42–73.
 70. Roy K, Ting TCH, Lau HH, Lim JBP. Effect of thickness on the behaviour of axially loaded back-to-back cold-formed steel built-up channel sections - Experimental and numerical investigation. *Structures*. 2018;16(December 2017):327–46.
 71. Roy K, Ting TCH, Lau HH, Lim JBP. Nonlinear behaviour of back-to-back gapped built-up cold-formed steel channel sections under compression. *J*

- Constr Steel Res. 2018;147:257–76.
72. Meza FJ, Becque J, Hajirasouliha I. Experimental study of cold-formed steel built-up columns. *Thin-Walled Struct* [Internet]. 2020;149(February):106291. Available from: <https://doi.org/10.1016/j.tws.2019.106291>
 73. Meza FJ, Becque J, Hajirasouliha I. Experimental study of the cross-sectional capacity of cold-formed steel built-up columns. *Thin-Walled Struct* [Internet]. 2020;155(July):106958. Available from: <https://doi.org/10.1016/j.tws.2020.106958>
 74. Muthuraman M, Anuradha R, Awoyera PO, Gobinath R. Numerical simulation and specification provisions for buckling characteristics of a built-up steel column section subjected to axial loading. *Eng Struct* [Internet]. 2020;207(December 2019):110256. Available from: <https://doi.org/10.1016/j.engstruct.2020.110256>
 75. Anbarasu M, Kanagarasu K, Sukumar S. Investigation on the behaviour and strength of cold-formed steel web stiffened built-up battened columns. *Mater Struct*. 2015 Dec 8;48(12):4029–38.
 76. Vijayanand S, Anbarasu M. Behavior of CFS built-up battened columns: Parametric study and design recommendations. *Struct Eng Mech*. 2020 May 10;74(3):381–94.
 77. Anbarasu M, Kumar SB, Sukumar S. Study on the effect of ties in the intermediate length Cold Formed Steel (CFS) columns. *Struct Eng Mech* [Internet]. 2013;46(3):323–35. Available from: <https://www.dbpia.co.kr/Journal/articleDetail?nodeId=NODE10233615>
 78. Dar MA, Sahoo DR, Jain AK, Sharma S. Monotonic tests and numerical validation of cold-formed steel battened built-up columns. *Thin-Walled Struct* [Internet]. 2021;159(October 2020):107275. Available from: <https://doi.org/10.1016/j.tws.2020.107275>
 79. Rahnavard R, Craveiro HD, Laím L, Simões RA, Napolitano R. Numerical investigation on the composite action of cold-formed steel built-up battened columns. *Thin-Walled Struct* [Internet]. 2021;162(February):107553. Available from: <https://doi.org/10.1016/j.tws.2021.107553>
 80. Abolhassan Astaneh-Asl, 1 A. M. ASCE, Subhash C. Goel, 2 and Robert D. Hanson, 3 Members A. Cyclic Out-of-Plane Buckling of Double-Angle Bracing. *J Struct Eng*. 1985;

81. Hosseini Hashemi B, Jafari MA. Experimental evaluation of cyclic behavior of batten columns. *J Constr Steel Res* [Internet]. 2012;78:88–96. Available from: <http://dx.doi.org/10.1016/j.jcsr.2012.06.014>
82. Poursamad Bonab A, Hosseini Hashemi B. Analytical investigation of cyclic behavior of laced built-up columns. *J Constr Steel Res* [Internet]. 2012;73(7):128–38. Available from: <http://dx.doi.org/10.1016/j.jcsr.2012.02.005>
83. Hosseini Hashemi B, Poursamad Bonab A. Experimental investigation of the behavior of laced columns under constant axial load and cyclic lateral load. *Eng Struct* [Internet]. 2013;57:536–43. Available from: <http://dx.doi.org/10.1016/j.engstruct.2013.09.033>
84. Kalochairetis KE, Gantes CJ, Lignos XA. Experimental and numerical investigation of eccentrically loaded laced built-up steel columns. *J Constr Steel Res* [Internet]. 2014 Oct [cited 2019 Oct 1];101:66–81. Available from: <https://linkinghub.elsevier.com/retrieve/pii/S0143974X14001242>
85. Biabannavard M, Behnamfar F, Zibasokhan H. Cyclic Behavior of Battened and Latticed Columns and Proposing a Substitute Super- Element. *Amirkabir J Civ Eng*. 2018;50(1):35–8.
86. BSI. Structural use of steelwork in building. Part [Internet]. 1985;3(1). Available from: http://www.sefindia.org/forum/files/bs5950_4_156.pdf
87. CSA.1989. Limit State Design of Steel Structure. CAN/CSA S161-M89 Can Stand Assoc. 1989;
88. Espinos A, Romero ML, Serra E, Hospitaler A. Experimental investigation on the fire behaviour of rectangular and elliptical slender concrete-filled tubular columns. *Thin-Walled Struct* [Internet]. 2015;93:137–48. Available from: <http://dx.doi.org/10.1016/j.tws.2015.03.018>
89. Portolés JM, Romero ML, Bonet JL, Filippou FC. Experimental study of high strength concrete-filled circular tubular columns under eccentric loading. *J Constr Steel Res* [Internet]. 2011;67(4):623–33. Available from: <http://dx.doi.org/10.1016/j.jcsr.2010.11.017>
90. Vernardos S, Gantes C. Experimental behavior of concrete-filled double-skin steel tubular (CFDST) stub members under axial compression: A comparative review. *Structures* [Internet]. 2019;22(October):383–404. Available from: <https://doi.org/10.1016/j.istruc.2019.06.025>

91. Han LH, Li W, Bjorhovde R. Developments and advanced applications of concrete-filled steel tubular (CFST) structures: Members. *J Constr Steel Res* [Internet]. 2014 [cited 2019 Nov 14];100:211–28. Available from: <http://dx.doi.org/10.1016/j.jcsr.2014.04.016>
92. Liu J, Yang Y, Liu J, Zhou X. Experimental investigation of special-shaped concrete-filled steel tubular column to steel beam connections under cyclic loading. *Eng Struct*. 2017 Nov 15;151:68–84.
93. Zhang D, Gao S, Gong J. Seismic behaviour of steel beam to circular CFST column assemblies with external diaphragms. *J Constr Steel Res*. 2012 Sep;76:155–66.
94. Yu Q, Tao Z, Wu YX. Experimental behaviour of high performance concrete-filled steel tubular columns. *Thin-Walled Struct*. 2008 Apr;46(4):362–70.
95. Roeder CW, Lehman DE, Bishop E. Strength and stiffness of circular concrete-filled tubes. *J Struct Eng*. 2010;136(12):1545–53.
96. Skalomenos KA, Hatzigeorgiou GD, Beskos DE. Parameter identification of three hysteretic models for the simulation of the response of CFT columns to cyclic loading. *Eng Struct* [Internet]. 2014;61:44–60. Available from: <http://dx.doi.org/10.1016/j.engstruct.2014.01.006>
97. Han LH, Yang YF. Cyclic performance of concrete-filled steel CHS columns under flexural loading. *J Constr Steel Res*. 2005;61(4):423–52.
98. Han LH, Huang H, Zhao XL. Analytical behaviour of concrete-filled double skin steel tubular (CFDST) beam-columns under cyclic loading. *Thin-Walled Struct*. 2009;47(6–7):668–80.
99. Han LH, Tao Z, Huang H, Zhao XL. Concrete-filled double skin (SHS outer and CHS inner) steel tubular beam-columns. *Thin-Walled Struct*. 2004;42(9):1329–55.
100. Lu H, Han LH, Zhao XL. Fire performance of self-consolidating concrete filled double skin steel tubular columns: Experiments. *Fire Saf J* [Internet]. 2010;45(2):106–15. Available from: <http://dx.doi.org/10.1016/j.firesaf.2009.12.001>
101. Romero ML, Espinos A, Portolés JM, Hospitaler A, Ibañez C. Slender double-tube ultra-high strength concrete-filled tubular columns under ambient temperature and fire. *Eng Struct* [Internet]. 2015;99:536–45. Available from:

<http://dx.doi.org/10.1016/j.engstruct.2015.05.026>

102. Hunaiti YM. Bond Strength in Battened Composite Columns. *J Struct Eng*. 1991;117(3):699–714.
103. Bambach MR, Jama H, Zhao XL, Grzebieta RH. Hollow and concrete filled steel hollow sections under transverse impact loads. *Eng Struct*. 2008;30(10):2859–70.
104. Szmigiera E, Zoltowski W, Siennicki M. Research on load capacity of concrete filled columns with battened steel sections. *J Civ Eng Manag* [Internet]. 2010 [cited 2019 Oct 29];16(3):313–9. Available from: <https://www.tandfonline.com/action/journalInformation?journalCode=tcem20>
105. Xu W, Han LH, Tao Z. Flexural behaviour of curved concrete filled steel tubular trusses. *J Constr Steel Res*. 2014;93:119–34.
106. Ahmed M, Liang QQ, Patel VI, Hadi MNS. Nonlinear analysis of rectangular concrete-filled double steel tubular short columns incorporating local buckling. *Eng Struct* [Internet]. 2018;175(June):13–26. Available from: <https://doi.org/10.1016/j.engstruct.2018.08.032>
107. EUROPEAN STANDARD. EN 1994-1-1 Design of composite steel and concrete structures. 2004;1(2005).
108. ACI 318-11. Building code requirements for structural concrete (ACI318-11). Vol. 2007, American Concrete Institute. 2011. 509 p.
109. Yoshiaki Goto MAGPKNK. Nonlinear Finite-Element Analysis for Hysteretic Behavior of Thin-Walled Circular Steel Columns with In-Filled Concrete. *J Struct Eng*. 2010;136(11).
110. Goto Y, Jiang K, Obata M. Stability and ductility of thin-walled circular steel columns under cyclic bidirectional loading. *J Struct Eng*. 2006;132(10):1621–31.
111. Patel VI, Liang QQ, Hadi MNS. Numerical analysis of high-strength concrete-filled steel tubular slender beam-columns under cyclic loading. *J Constr Steel Res*. 2014;92:183–94.
112. Razzaghi MS, Khalkhaliha M, Aziminejad A. Cyclic performance of concrete-filled steel batten built-up columns. *Int J Adv Struct Eng*. 2016;8(1):45–51.
113. Seica M V., Packer JA. FRP materials for the rehabilitation of tubular steel structures, for underwater applications. *Compos Struct*. 2007;80(3):440–50.

114. Tao Z, Han LH, Zhuang JP. Axial loading behavior of CFRP strengthened concrete-filled steel tubular stub columns. *Adv Struct Eng.* 2007;10(1):37–46.
115. Yu T, Hu YM, Teng JG. FRP-confined circular concrete-filled steel tubular columns under cyclic axial compression. *J Constr Steel Res.* 2014;94:33–48.
116. Hu YM, Yu T, Teng JG. FRP-Confined Circular Concrete-Filled Thin Steel Tubes under Axial Compression. *J Compos Constr.* 2011;15(5):850–60.
117. Feng P, Zhang Y, Bai Y, Ye L. Combination of Bamboo Filling and FRP Wrapping to Strengthen Steel Members in Compression. *J Compos Constr.* 2013;17(3):347–56.
118. Feng P, Zhang Y, Bai Y, Ye L. Strengthening of steel members in compression by mortar-filled FRP tubes. *Thin-Walled Struct* [Internet]. 2013;64:1–12. Available from: <http://dx.doi.org/10.1016/j.tws.2012.11.001>
119. Selvaraj S, Madhavan M. Strengthening of unsymmetrical open channel built-up beams using CFRP. *Thin-Walled Struct.* 2017;119(September 2016):615–28.
120. Selvaraj S, Madhavan M. Enhancing the structural performance of steel channel sections by CFRP strengthening. *Thin-Walled Struct.* 2016 Nov;108:109–21.
121. Selvaraj S, Madhavan M, Dongre SU. Experimental Studies on Strength and Stiffness Enhancement in CFRP-Strengthened Structural Steel Channel Sections under Flexure. *J Compos Constr* [Internet]. 2016 Dec;20(6):04016042. Available from: <http://ascelibrary.org/doi/10.1061/%28ASCE%29CC.1943-5614.0000700>
122. Selvaraj S, Madhavan M. CFRP strengthened steel beams: Improvement in failure modes and performance analysis. *Structures.* 2017 Nov;12(August):120–31.
123. Tafsirojjaman T, Fawzia S, Thambiratnam DP, Zhao XL. FRP strengthened SHS beam-column connection under monotonic and large-deformation cyclic loading. *Thin-Walled Struct* [Internet]. 2021;161(January):107518. Available from: <https://doi.org/10.1016/j.tws.2021.107518>
124. Tafsirojjaman T, Fawzia S, Thambiratnam DP. Structural behaviour of CFRP strengthened beam-column connections under monotonic and cyclic loading. *Structures* [Internet]. 2021;33(May):2689–99. Available from: <https://doi.org/10.1016/j.istruc.2021.06.028>

125. Kalavagunta S, Naganathan S, Mustapha KN Bin. Axially loaded steel columns strengthened with CFRP. *Jordan J Civ Eng.* 2014;8(1):58–69.
126. Mohamed HM, Ali AH, Benmokrane B. Behavior of Circular Concrete Members Reinforced with Carbon-FRP Bars and Spirals under Shear. *J Compos Constr.* 2017;21(2):04016090.
127. Hajarul Falahi Abdul Halim N, Alih SC, Vafaei M. Comparison between cyclic response of RC columns transversely reinforced with FRP strips and carbon steel. *IOP Conf Ser Mater Sci Eng.* 2019;513(1).
128. Soudki K, Alkhrdaji T. Guide for the Design and Construction of Externally Bonded FRP Systems for Strengthening Concrete Structures (ACI 440.2R-02). *Proceedings of the Structures Congress and Exposition.* 2005. 1627–1633 p.
129. ISIS C (2001). Strengthening reinforced concrete structures with externally bonded fibre reinforced polymers. ISIS Canada; 2001.
130. (JSCE) JS of CE. Recommendations for upgrading of concrete structures with use of continuous fiber sheets. *Concrete engineering.* 2001.
131. Alkhrdaji T. Strengthening of Concrete Structures Using FRP Composites. *Struct Mag [Internet].* 2015;(June):18–20. Available from: <https://www.structuremag.org/wp-content/uploads/2015/05/C-BuildingBlocks-Alkhrdaji-Jun151.pdf> %0Ahttp://www.structuremag.org/
132. Horse. FRP strengthening concrete beam, column and slab [Internet]. Available from: <https://www.fibermaxcomposites.com/shop/carbon-fiber-fabric-br-c80u-p-100076.html?cPath=36>
133. Sen R, Liby L. Repair of Steel Composite Bridge Sections using Carbon Fiber Reinforced Plastic Laminates-restraint Effect of Bearings-phase ii. 1994.
134. Mertz DR, Gillespie Jr JW. Rehabilitation of steel bridge girders through the application of advanced composite materials. 1996.
135. Ekiz E, El-Tawil S. Restraining Steel Brace Buckling Using a Carbon Fiber-Reinforced Polymer Composite System: Experiments and Computational Simulation. *J Compos Constr.* 2008;12(5):562–9.
136. Bambach MR, Jama HH, Elchalakani M. Axial capacity and design of thin-walled steel SHS strengthened with CFRP. *Thin-Walled Struct [Internet].* 2009;47(10):1112–21. Available from:

<http://dx.doi.org/10.1016/j.tws.2008.10.006>

137. Sayed-Ahmed EY, Shaat AA, Abdallah EA. CFRP-Strengthened HSS Columns Subject to Eccentric Loading. *J Compos Constr.* 2018;22(4):04018025.
138. Naganathan S, Chakravarthy HGN, Anuar NA, Kalavagunta S, Mustapha KN Bin. Behaviour of Cold Formed Steel Built-Up Channel Columns Strengthened Using CFRP. *Int J Steel Struct [Internet].* 2020;20(2):415–24. Available from: <https://doi.org/10.1007/s13296-019-00293-5>
139. Liang J, Lin S, Li W, Liu D. Axial compressive behavior of recycled aggregate concrete-filled square steel tube stub columns strengthened by CFRP. *Structures [Internet].* 2021;29(November 2020):1874–81. Available from: <https://doi.org/10.1016/j.istruc.2020.12.084>
140. Tang Y, Fang S, Chen J, Ma L, Li L, Wu X. Axial compression behavior of recycled-aggregate-concrete-filled GFRP–steel composite tube columns. *Eng Struct [Internet].* 2020;216(January):110676. Available from: <https://doi.org/10.1016/j.engstruct.2020.110676>
141. Du Y, Zhang Y, Chen Z, Yan J-B, Zheng Z. Axial compressive performance of CFRP confined rectangular CFST columns using high-strength materials with moderate slenderness. *Constr Build Mater [Internet].* 2021;299:123912. Available from: <https://doi.org/10.1016/j.conbuildmat.2021.123912>
142. Jian X, Liu H, Zhao Z, Wu X, Lei M, Chen Z. A study of the mechanical behavior of rectangular steel tubular column strengthened using intermittent welding angle steel. *Structures [Internet].* 2021;33(June):3298–310. Available from: <https://doi.org/10.1016/j.istruc.2021.06.031>
143. Selvaraj S, Madhavan M. Retrofitting of Structural Steel Channel Sections Using Cold-Formed Steel Encasing Channels. *J Perform Constr Facil.* 2018;32(4):04018049.
144. Adil Dar M, Subramanian N, Manzoor Z, Fayeeg Ghowsi A, Carvalho H, Dar AR. Retrofitting of Hot-Rolled Steel Channels Using CFS Sections: Experimental Study and Flexural Behavior. *Pract Period Struct Des Constr.* 2020;25(4):04020038.
145. Tafsirojjaman, Fawzia S, Thambiratnam D, Zhao XL. Behaviour of CFRP strengthened CHS members under monotonic and cyclic loading. *Compos Struct [Internet].* 2019;220(February):592–601. Available from:

- <https://doi.org/10.1016/j.compstruct.2019.04.029>
146. Tafsirojjaman T, Fawzia S, Thambiratnam DP, Zhao XL. Study on the cyclic bending behaviour of CFRP strengthened full-scale CHS members. Structures [Internet]. 2020;28(July):741–56. Available from: <https://doi.org/10.1016/j.istruc.2020.09.015>
 147. Tafsirojjaman T, Fawzia S, Thambiratnam D, Zhao XL. Numerical investigation of CFRP strengthened RHS members under cyclic loading. Structures [Internet]. 2020;24(November 2019):610–26. Available from: <https://doi.org/10.1016/j.istruc.2020.01.041>
 148. Mahin SA. Lessons from damage to steel buildings during the Northridge earthquake. Eng Struct. 1998;20(4–6):261–70.
 149. Tafsirojjaman, Fawzia S, Thambiratnam D. Enhancement of seismic performance of steel frame through CFRP strengthening. Procedia Manuf [Internet]. 2019;30:239–46. Available from: <https://doi.org/10.1016/j.promfg.2019.02.035>
 150. Chen Z, Dong S, Du Y. Experimental study and numerical analysis on seismic performance of FRP confined high-strength rectangular concrete-filled steel tube columns. Thin-Walled Struct [Internet]. 2021;162(September 2020):107560. Available from: <https://doi.org/10.1016/j.tws.2021.107560>
 151. Zeinoddini M, Parke GAR, Harding JE. Axially pre-loaded steel tubes subjected to lateral impacts: An experimental study. Int J Impact Eng. 2002;27(6):669–90.
 152. Alam MI, Fawzia S. Numerical studies on CFRP strengthened steel columns under transverse impact. Compos Struct [Internet]. 2015;120:428–41. Available from: <http://dx.doi.org/10.1016/j.compstruct.2014.10.022>
 153. Alam I, Fawzia S, Zhao X, Asce F, Remennikov AM. Experimental Study on FRP-Strengthened Steel Tubular Members under Lateral Impact. J Compos Constr. 2013;
 154. Computers and Structures Inc. C. SAP2000: Integrated Finite Element Analysis and Design of Structures. Berkeley; 2020.
 155. Han LH, Yang YF, Tao Z. Concrete-filled thin-walled steel SHS and RHS beam-columns subjected to cyclic loading. Thin-Walled Struct. 2003 Sep;41(9):801–33.
 156. FEMA 461. Interim Testing Protocols for Determining the Seismic

- Performance Characteristics of Structural and Nonstructural Components. 2007;(June).
157. ISO 17025. International Standard ISO / IEC competence of testing and calibration. *Int Organ Stand* [Internet]. 2017;2017:1–38. Available from: <https://www.iso.org/fr/standard/39883.html>
 158. ASTM A370/ ASME A-730 2004. *Astm a370 / Asme Sa-370*. *ASTM Int*. 2004;155(23):739–44.
 159. Test CC, Drilled T, Elements C, Drilled U, Cores C, Concrete C. Standard Test Method for Static Modulus of Elasticity and Poisson ' s Ratio of Concrete. 2006;2–6.
 160. ACI 440.2R-17. Guide for the Design and Construction of Externally Bonded FRP Systems for Strengthening Concrete Structures. 440.2R-17: Guide for the Design and Construction of Externally Bonded FRP Systems for Strengthening Concrete Structures. 2017.
 161. Della Corte G, Landolfo R. Lateral loading tests of built-up battened columns with semi-continuous base-plate connections. *J Constr Steel Res* [Internet]. 2017 Nov [cited 2019 Apr 11];138:783–98. Available from: <https://linkinghub.elsevier.com/retrieve/pii/S0143974X17306016>
 162. FEMA P. Commentary for the Seismic Rehabilitation of Buildings. FEMA-356, Fed Emerg Manag Agency, Washington, DC. 2000;(1):1–518.
 163. Song S, Wang G, Min X, Duan N, Tu Y. Experimental study on cyclic response of concrete frames reinforced by Steel-CFRP hybrid reinforcement. *J Build Eng* [Internet]. 2021;34(April):101937. Available from: <https://doi.org/10.1016/j.jobbe.2020.101937>
 164. Teng JG, Hu YM. Behaviour of FRP-jacketed circular steel tubes and cylindrical shells under axial compression. *Constr Build Mater*. 2007;21(4):827–38.
 165. Yu T, Hu YM, Teng JG. Cyclic lateral response of FRP-confined circular concrete-filled steel tubular columns. *J Constr Steel Res*. 2016;124:12–22.
 166. Li LJ, Fang S, Fu B, Chen HD, Geng MS. Behavior of hybrid FRP-concrete-steel multitube hollow columns under axial compression. *Constr Build Mater*. 2020;253.
 167. Simulia DCS (2014). ABAQUS 6.14 Analysis User's Manual: Getting Started with Abaqus Interactive Edition. 2014.

168. Budaházy V, Dunai L. Parameter-refreshed Chaboche model for mild steel cyclic plasticity behaviour. *Period Polytech Civ Eng.* 2013;57(2):139–55.
169. Shi Y, Wang M, Wang Y. Experimental and constitutive model study of structural steel under cyclic loading. *J Constr Steel Res* [Internet]. 2011;67(8):1185–97. Available from: <http://dx.doi.org/10.1016/j.jcsr.2011.02.011>
170. Shen C, Mamaghani IHP, Mizuno E, Usami T. Cyclic behavior of structural steels. II: Theory. *J Eng Mech.* 1995;121(11):1165–72.
171. White DW, Mc Guire W. Uniaxial cyclic stress-strain behavior of structural steel. Vol. 113, *Journal of Engineering Mechanics.* 1987. p. 1803–5.
172. SHEN C, TANAKA Y, MIZUNO E, USAMI T. A Two-Surface Model for Steels with Yield Plateau. *Doboku Gakkai Ronbunshu.* 1992;8(441):11–20.
173. Chaboche JL. Time-independent constitutive theories for cyclic plasticity. *Int J Plast.* 1986;2(2):149–88.
174. Jia L, Kuwamura H. Prediction of Cyclic Behaviors of Mild Steel at Large Plastic Strain Using Coupon Test Results. *J Struct Eng.* 2014;140(2):04013056.
175. Zhou H, Wang Y, Shi Y, Xiong J, Yang L. Extremely low cycle fatigue prediction of steel beam-to-column connection by using a micro-mechanics based fracture model. *Int J Fatigue.* 2013 Mar;48:90–100.
176. Huang Z, Li D, Uy B, Thai HT, Hou C. Local and post-local buckling of fabricated high-strength steel and composite columns. *J Constr Steel Res.* 2019 Mar 1;154:235–49.
177. Liang QQ. Performance-based analysis of concrete-filled steel tubular beam-columns, Part I: Theory and algorithms. *J Constr Steel Res* [Internet]. 2009;65(2):363–72. Available from: <http://dx.doi.org/10.1016/j.jcsr.2008.03.007>
178. Liu Q, Zhou D, Wang J, Liu W. Mechanical behavior of FRP confined steel tubular columns under impact. *Steel Compos Struct.* 2018;27(6):691–702.
179. Wang Z Bin, Tao Z, Han LH, Uy B, Lam D, Kang WH. Strength, stiffness and ductility of concrete-filled steel columns under axial compression. *Eng Struct.* 2017 Mar 15;135:209–21.
180. Rabbat BG, Russell HG. Friction coefficient of steel on concrete or grout. *J Struct Eng (United States).* 1985;111(3):505–15.

181. Song Y, Li J, Chen Y. Local and post-local buckling of normal/high strength steel sections with concrete infill. *Thin-Walled Struct.* 2019 May 1;138:155–69.
182. Tan JK, Wang YH, Su MN, Zhang H Bin, Peng YY. Compressive behaviour of built-up hot-rolled steel hollow and composite sections. *Eng Struct.* 2019 Nov 1;198.
183. Schneider SP. Axially Loaded Concrete-Filled Steel Tubes. *J Struct Eng.* 1998;124(10):1125–38.
184. Lam D, Dai XH, Han LH, Ren QX, Li W. Behaviour of inclined, tapered and STS square CFST stub columns subjected to axial load. *Thin-Walled Struct.* 2012;54:94–105.
185. Vasdravellis G, Uy B, Tan EL, Kirkland B. Behaviour and design of composite beams subjected to negative bending and compression. *J Constr Steel Res.* 2012;79:34–47.
186. Bursi OS, Jaspart JP. Basic issues in the finite element simulation of extended end plate connections. *Comput Struct.* 1998;69(3):361–82.
187. Spring N. Obtaining a Converged Solution with Abaqus. *Dassault Systèmes;* 2010. p. 456.
188. Tao Z, Mirza O, Song T, Han L. Finite Element Analysis of Steel Beam-Cfst Column Joints With Blind Bolts. *Australas Struct Eng 2014 Conf (ASEC 2014).* 2014;(July):56(1-10).
189. H HR, S VK, Kumar R, Sklyut H, Kulak M, Heinimann M. Performance Evaluation of Finite Elements for Analysis of Advanced Hybrid Laminates. *SIMULIA Cust Conf.* 2010;1–15.
190. Kazemzadeh Azad S, Uy B. Effect of concrete infill on local buckling capacity of circular tubes. *J Constr Steel Res [Internet].* 2020 [cited 2020 Mar 3];165. Available from: <https://doi.org/10.1016/j.jcsr.2019.105899>
191. Ellobody E, Young B. Behavior of cold-formed steel plain angle columns. *J Struct Eng.* 2005;131(3):457–66.
192. Yu C, Schafer BW. Effect of longitudinal stress gradient on the ultimate strength of thin plates. *Thin-Walled Struct.* 2006;44(7):787–99.
193. Yu C, Schafer BW. Effect of Longitudinal Stress Gradients on Elastic Buckling of Thin Plates. *J Eng Mech [Internet].* 2007 Apr;133(4):452–63. Available from: <http://ascelibrary.org/doi/10.1061/%28ASCE%290733->

9399%282007%29133%3A4%28452%29

194. Morales EM. Significance of the Ratio of Tensile Strength To Yield Stress (Ts/Ys) of Reinforcing Bars. CAST '98 Conf Concr Art, Sci Technol [Internet]. 1998; Available from: internal-pdf://131.89.193.131/Morales.PDF
195. Morales BEM, Cruz JEJ. “ Stronger Is Not Necessarily Better ” - The Significance of Tests and Properties of Civil Engineering Materials. :1–14.
196. ASCE/SEI 7-10. ASCE Standard Loads for Buildings. Minimum Design Loads for Buildings and Other Structures. 2016. 253 p.

LIST OF PUBLICATIONS

1. A. Waheed, M. Vafaei, S. C. Alih, R. Ullah, Experimental and numerical investigations on the seismic response of built-up battened columns, *J. Constr. Steel Res.* 174 (2020) 106296. <https://doi.org/10.1016/j.jcsr.2020.106296>.
2. A. Waheed, M. Vafaei, S. C. Alih, R. Ullah, Effect of battens' spacing on the cyclic response of built-up columns, *Thin-Walled Structure Res.* 172 (2022) 108862 <https://doi.org/10.1016/j.tws.2021.108862>